NAVAL POSTGRADUATE SCHOOL
Monterey, California

THESIS

The Effect of Rician Fading and Partial-Band Interference on Noise-Normalized Fast Frequency-Hopped MFSK Receivers

by

Melody Kragh

March 1994

Thesis Advisor: R. Clark Robertson
Second Reader: Ron J. Pieper

Approved for public release, distribution is unlimited.

REPORT DOCUMENTATION PAGE

Form Approved
OMB No. 0704-0188

1. AGENCY USE ONLY (Leave blank)	2. REPORT DATE	3. REPORT TYPE AND DATES COVERED
	March 1994	Master's Thesis

4. TITLE AND SUBTITLE
THE EFFECT OF RICIAN FADING AND PARTIAL-BAND INTERFERENCE ON NOISE-NORMALIZED FAST FREQUENCY-HOPPED MFSK RECEIVERS

5. FUNDING NUMBERS

6. AUTHOR(S)
Kragh, Melody

7. PERFORMING ORGANIZATION NAME(S) AND ADDRESS(ES)
Naval Postgraduate School
Monterey, CA 93943-5000

8. PERFORMING ORGANIZATION REPORT NUMBER

9. SPONSORING / MONITORING AGENCY NAME(S) AND ADDRESS(ES)

10. SPONSORING / MONITORING AGENCY REPORT NUMBER

11. SUPPLEMENTARY NOTES
The views expressed in this thesis are those of the author and do not reflect the official policy or position of the Department of Defense or the United States Government.

12a. DISTRIBUTION / AVAILABILITY STATEMENT
Approved for public release; distribution unlimited.

12b. DISTRIBUTION CODE
A

13. ABSTRACT (Maximum 200 words)
The performance of an M-ary orthogonal frequency-shift keying (MFSK) communication system employing fast frequency-hopped spread spectrum waveforms transmitted over a frequency-nonselective, slowly fading channel with partial-band interference is analyzed. A procedure referred to as noise-normalization combining is employed by the system receiver to minimize partial-band interference effects. Each hop is assumed to fade independently. The partial-band interference is modeled as a Gaussian process. Both the signal and the partial-band interference are assumed to be affected by the fading channel which is modeled as Rician. The effect of fading of the partial-band interference on worst-case receiver performance is relatively minor. When there is no signal fading or when the signal fading is Rician, then the counter-intuitive result of poorer receiver performance when the partial-band interference experiences fading is obtained. This effect is most pronounced when the signal does not fade and the partial-band interference experiences Rayleigh fading.

14. SUBJECT TERMS	15. NUMBER OF PAGES
communications, noise-normalized receiver, noncoherent receiver, spread spectrum, FFH, M-ary FSK	72
	16. PRICE CODE

17. SECURITY CLASSIFICATION OF REPORT	18. SECURITY CLASSIFICATION OF THIS PAGE	19. SECURITY CLASSIFICATION OF ABSTRACT	20. LIMITATION OF ABSTRACT
UNCLASSIFIED	UNCLASSIFIED	UNCLASSIFIED	UL

Approved for public release; distribution is unlimited

The Effect of Rician Fading and Partial-Band Interference on Noise-Normalized Fast Frequency-Hopped MFSK Receivers

by

Melody Kragh
Lieutenant, United States Navy
B. S., California State University at Sacramento, 1987

Submitted in partial fulfillment of the
requirements for the degree of

MASTER OF SCIENCE IN ELECTRICAL ENGINEERING

from the

NAVAL POSTGRADUATE SCHOOL

March 1994

Author: Melody Kragh
Melody Kragh

Approved by: R. Clark Robertson
R. Clark Robertson, Thesis Advisor

Ron J. Pieper
Ron J. Pieper, Second Reader

Michael A. Morgan
Michael A. Morgan, Chairman, Department of Electrical and Computer Engineering

ABSTRACT

The performance of an M-ary orthogonal frequency-shift keying (MFSK) noncoherent communication system employing fast frequency-hopped spread spectrum waveforms transmitted over a frequency-nonselective, slowly fading channel with partial-band interference is analyzed. A procedure referred to as noise-normalization combining is employed by the system receiver to minimize partial-band interference effects. Each hop is assumed to fade independently. The partial-band interference is modeled as a Gaussian process. Both the signal and the partial-band interference are assumed to be affected by the fading channel which is modeled as Rician. The effect of fading of the partial-band interference on worst-case receiver performance is relatively minor. When there is no signal fading or when the signal fading is Rician, then the counter-intuitive result of poorer receiver performance when the partial-band interference experiences fading is obtained. This effect is most pronounced when the signal does not fade and the partial-band interference experiences Rayleigh fading.

TABLE OF CONTENTS

LIST OF FIGURES

ACKNOWLEDGMENT

I thank God for all the times He carried me, gave me strength, and inspired me to finish this thesis, even when intermediate results appeared discouraging. I thank my advisor, Professor R. Clark Robertson for his guidance, insight, patience, and friendship. I thank my son, Michael, who brings joy into my life, for his tolerance and for drawing me back into family life when I became too involved in this thesis. And lastly, I thank my husband for his proof reading, perspective, and empathy.

I. INTRODUCTION

Spread spectrum is a communication modulation technique used both for commercial and military communications. The commercial users are primarily concerned with multiple access to the same frequency bandwidth due to bandwidth limitations. The military users are primarily concerned with transmission security. Transmission security includes the reduction of a hostile user's ability to intercept the transmission, to detect the transmission, or to jam the transmission [1, 2].

Direct sequence, frequency-hopping, and time-hopping are common spread spectrum techniques; direct sequence, frequency-hopping, and hybrid direct sequence, frequency-hopped systems are the most commonly used. Direct sequence spread spectrum modulation affords a low probability of detection by spreading the signal power over a much wider bandwidth. In frequency-hopping spread spectrum modulation, the carrier frequency is continually switched pseudorandomly over a large bandwidth resulting in a low probability of interception. Both of these types of spread spectrum systems reduce the effectiveness of hostile jamming. Hybrid direct sequence, frequency-hopped systems combine direct sequence and frequency-hopping by generating a direct sequence signal that is then frequency-hopped. Hybrid systems are capable of a wider bandwidth than can be obtained by either system alone and offer both low probability of detection and low probability of interception. This combination of characteristics is classified as low probability of exploitation [2, 3, 4].

For a frequency-hopped spread spectrum system, if more than one symbol is transmitted per frequency hop, the system is classified as a slow frequency-hopped system. If the hop rate is equal to or greater than the symbol rate, producing one

or more hop per symbol, the system is classified as fast frequency-hopped. Fast frequency-hopped spread spectrum signals reduce a jammer's ability to interfere with the signal's transmission. Ideally, the communication must seem complex and random to the jammer and completely deterministic to the intended receiver. A block diagram of a frequency-hopping system is shown in Fig. 1 [2] [3, 4, 5].

Binary or M-ary frequency-shift keying (FSK) is most frequently used with frequency-hopping spread spectrum, although other modulations such as binary phase-shift keying could in principle be employed. Typically phase recovery is impractical for modern frequency-hopped spread spectrum systems, with the result that only modulation schemes that can be demodulated noncoherently are employed. In contrast, direct sequence spread spectrum systems typically use either binary phase-shift keying (BPSK) or quadrature phase-shift keying (QPSK) and coherent detection.

In FSK the data determines the frequency of the signal sent as indicated in

$$\begin{aligned} s_m(t) &= A\cos[2\pi(f_c + m\Delta f)t] \quad \text{for} \quad 0 \le t \le T \\ \text{where } m &= 0, 1, 2, \cdots, M-1 \\ \Delta f &= \text{frequency separation} \\ &= \frac{n}{T} \text{ for orthogonal noncoherent FSK, } n = 1, 2, 3, \cdots \end{aligned} \tag{1}$$

The symbol energy, E_s, is

$$\begin{aligned} E_s &= \int_0^T s_m^2(t)dt \\ &= \int_0^T A^2\cos^2[2\pi(f_c + m\Delta f)t]\,dt \\ &= \frac{A^2}{2}\left\{1 + \frac{\sin[4\pi(f_c + m\Delta f)t]}{4\pi(f_c + m\Delta f)}\right\}\Bigg|_0^T \end{aligned} \tag{2}$$

$$= \frac{A^2T}{2}\left\{1+\frac{\sin\left[4\pi\left(f_c+m\Delta f\right)T\right]}{4\pi\left(f_c+m\Delta f\right)}\right\}$$

$$= \frac{A^2T}{2}\left(\text{assuming } f_c \gg \frac{1}{T} \quad \text{or} \quad \Delta f = \frac{n}{T},\ n=1,2,3,\cdots\right)$$

The number of bits required to represent a M-ary symbol is k, where $k = \log_2 M$ [3]. Thus, E_s is equal to k times the bit energy, E_b. The symbol rate, R_s, is equal to the bit rate, R_b, divided by k [2].

The transmitted signal might be reflected off surrounding objects as it travels to the receiver either in addition to or in place of a direct line-of-sight signal path. Therefore, the receiver may pick up a direct component of the signal, i.e., from the line-of-sight path and an indirect component from a reflected path as shown in Fig. 2. The indirect signal component, referred to also as multipath, may interfere constructively or destructively, thus, reducing receiver performance. This reduction in performance is called multipath fading [4, 6].

When the line-of-sight component of the received signal is zero, the received signal amplitude is modeled as a Rayleigh random variable, and the channel is called a Rayleigh fading channel. When the line-of-sight component is not zero, the received signal amplitude is modeled as a Ricean random variable, and the channel is called a Rician fading channel. Rician fading is more likely for the mobile user satellite communication, especially when either the transmitter or the receiver have highly directional antennas. Rayleigh fading is more likely in the case of mobile user ground station communication where a direct path between the transmitter and receiver may not exist [2, 7].

A jammer can interfere with the transmitted signal by transmitting power on the same frequency band. The jammer can either transmit a noise-like signal over the entire bandwidth, called barrage jamming, or transmit over a fraction of the bandwidth. This can consist of either tone jamming or partial-band noise

jamming. In response the transmitter can employ a repetition technique such as fast frequency-hopping, a form of diversity, to offset the effects of multipath fading and partial-band jamming. A noncoherent receiver can significantly decrease the advantage gained by diversity when fading is not present. The repeated signals, L, are received and combined out of phase (noncoherently) resulting in noncoherent combining losses. The coherent receiver does not suffer these losses; however, the coherent FSK receiver is not often employed because of the added complexity and expense [4, 8].

Depending on power constraints and system design, the transmitter can either use a constant energy per hop, E_H, or a constant energy per symbol, E_s, strategy. A constant E_H with increasing diversity implies an increase in E_s, since $E_s = LE_H = LE_H/k$ [5]. The choice also depends on the interference environment and the type of intended receiver.

The receiver can combine the outputs of the M branches of the receiver in either a linear or a nonlinear manner. A linear combining receiver is the easiest to analyze. The conventional FSK receiver utilizes linear combining and is shown in Fig. 3. A conventional receiver equally weights each hop of the received signal. If the interference noise is not considered an input to the system, then the noise-normalized receiver also ultilizes linear combining, however, each hop of the received signal is weighted differently depending on the level of jammer interference, thus better receiver performance is achieved. If a receiver can distinguish between jammed and unjammed hops it is said to have side information. This allows the receiver to give less weight to the jammed hops. If the side information is without error, called perfect side information, than the jammed hops can be ignored [4, 9].

In this thesis the performance of a noise-normalized, fast frequency-hopped M-ary orthogonal frequency-shift keying (FFH/MFSK) system with noncoherent

detection is analyzed. The FFH/MFSK transmitter is assumed to perform L hops per data symbol. At the receiver the dehopped signals are demodulated by two correlators in phase quadrature per signal waveform. The correlator outputs are sampled every T seconds where T is the symbol period. Since the carrier phases are not recovered, the sampled outputs of each correlator pair are squared and summed. The noise power of a noise-only channel estimator is used to normalize the output of each of the M branches of the MFSK demodulator before the L hop receptions are combined to form the decision statistics. A block diagram of the FFH/MFSK receiver with noise-normalization combining is shown in Fig. 4. An accurate measurement of the noise power present in each hop is a challenging problem in fast frequency-hopped spread spectrum systems. In order to perform a complete evaluation of the noise-normalized receiver, the effect of an inexact estimation of noise power on system performance should be examined [4]. The noise power is assumed to be estimated without error; hence, the performance obtained for the noise-normalized receiver in this thesis is in this sense ideal.

The communications channel is modeled as a fading channel, and the FFH/MFSK signal is assumed to be affected by partial-band interference in addition to standard additive white Gaussian noise. The effect of channel fading and partial-band interference on communications systems was initially investigated for standard noncoherent MFSK demodulators in [10]; and the effect of partial-band interference, but without channel fading, on noise-normalized FFH/MFSK demodulators was investigated in [11, 12]. More recently, the effect of both partial-band interference and channel fading on noise-normalized FFH/MFSK demodulators has been examined [13]. In previous work examining the effects of fading channels on system performance, it is assumed that only the communications signal is affected by fading. It seems reasonable that, in general, in situations where channel fading affects the com-

munications signal that it will also affect the partial-band interference signal. Hence, previous analyses that ignore the effect of fading on the partial-band interference yield, from the viewpoint of the communications system, overly pessimistic results. In this thesis, communications system performance when both the FFH/MFSK signal and the partial-band interference are affected by the fading channel is examined.

The partial-band interference that is considered here may be due to either a partial-band noise jammer or some unintended narrowband interference. The interference is modeled as additive Gaussian noise and, when present, is assumed to be in each branch of the MFSK demodulator for any reception of the dehopped signal. In addition to partial-band interference, the signal is also assumed to be corrupted by thermal noise and other wideband interferences which are modeled as additive white Gaussian noise. This wideband noise is assumed to be unaffected by the fading channel.

The narrowband interference for each hop and each dehopped signal are both assumed to fade independently. This implies that the smallest spacing between frequency hop slots is larger than the coherence bandwidth of the channel [8, 14, 15]. The channel for each hop is also modeled as a frequency-nonselective, slowly fading Rician process. This implies that the bandwidth of both the signal and the narrowband interference is much smaller than the coherence bandwidth of the channel and that the hop duration is much smaller than the coherence time of the channel [8, 14]. The latter assumption is equivalent to requiring the hop rate to be large compared to the Doppler spread of the channel. Consequently, both the dehopped signal amplitude and the amplitude of the partial-band interference signal can be modeled as independent Rician random variables where the total power in both the communication signal and the narrowband interference signal can

be considered as the sum of the power in a direct component and that in a diffuse component.

The bit rate is taken to be R_b. Hence, the corresponding symbol rate is $R_s = R_b/\log_2 M$ where M is the order of the MFSK modulation. Since the FFH/MFSK signal has L hops per symbol, the hop rate is $R_H = LR_s$.The equivalent noise bandwidth of noise-only channel estimator is B, where B is assumed to equal R_H. The overall system bandwidth is assumed to be very large compared to the hop rate. Note that for a fixed symbol rate that the hop rate increases as the number of hops per symbol increases. As a result, the required minimum equivalent noise bandwidth of the correlation detectors in the MFSK demodulator also increases as the number of hops per symbol increases. Hence, as the number of hops increases, the assumption that the channel is frequency-nonselective becomes more restrictive. On the other hand, the assumption that the channel is slowly fading becomes stronger.

(THIS PAGE INTENTIONALLY LEFT BLANK)

II. NOISE-NORMALIZED RECEIVER SYSTEM ANALYSIS

The partial-band interference is assumed to be present in each branch of the MFSK demodulator for any reception of the dehopped signal with probability γ. Thus, γ represents the fraction of the spread bandwidth being jammed, and the probability that narrowband interference is not present in all M detectors is $1-\gamma$. If $N_I/2$ is the average power spectral density of interference over the entire spread bandwidth, then $\gamma^{-1}N_I/2$ is the power spectral density of partial-band interference when it is present. The power spectral density of thermal noise and other wideband interferences, which is modeled as additive white Gaussian noise, is defined as $N_0/2$. Hence, the power spectral density of the total noise is $\gamma^{-1}N_I/2+N_0/2$ when partial-band interference is present and $N_0/2$ otherwise. If the equivalent noise bandwidth of each correlator in the noise-normalized MFSK demodulator is B Hz, then for each hop each correlator output has noise of power N_0B with probability $1-\gamma$when interference is not present and noise of power $(\gamma^{-1}N_I+N_0)B$ with probability γ when interference is present. Hence, the noise power in a given hop k of a symbol is defined

$$\sigma_k^2 = \left\{ \begin{array}{ll} \sigma_T^2+\sigma_I^2 & \text{with probability } \gamma \\ \sigma_T^2 & \text{with probability } 1-\gamma \end{array} \right\} \tag{3}$$

where $\sigma_T^2 = N_0B$ and $\sigma_I^2 = \gamma^{-1}N_IB$.

A. PROBABILITY OF BIT ERROR

The probability of symbol error for the receiver in Fig. 1 when partial-band interference is present is [2]

$$P_s = \sum_{i=0}^{L} \left(\begin{array}{c} L \\ i \end{array} \right) \gamma^i(1-\gamma)^{L-i}P_s(i) \tag{4}$$

where $P_s(i)$ is the conditional probability symbol error given that i hops of a symbol have interference. Due to the symmetric structure of the receiver, $P_s(i)$ can be obtained by considering only the case where the signal is present in branch 1 of the MFSK demodulator. The outputs of each channel not containing the signal are assumed identical and independent.

For orthogonal MFSK the probability of bit error is related to the probability of symbol error by [2]

$$P_b = \frac{M}{2(M-1)} P_s \tag{5}$$

The energy per bit is related to the symbol energy, E_s, by

$$E_b = \frac{E_s}{\log_2 M} \tag{6}$$

and the energy per bit is related to the energy per hop, E_H, by

$$E_b = LE_H \tag{7}$$

In this case, Z_1 is the random variable conditioned on i of L hops having interference that represents the output of the demodulator branch containing the signal after the noise normalization operation and after the combining of each hop of a symbol. The random variables $Z_m, m = 2, 3, \cdots, M$ represent the outputs of the demodulator branches that do not contain a signal after the noise normalization operation and after the combining of each hop of a symbol. Given the conditional probability density functions $f_{Z_1}(z_1|i)$ and $f_{Z_m}(z_m), m = 2, 3, \cdots, M$, the probability for symbol error is [2]

$$P_s(i) = 1 - \int_0^\infty f_{Z_1}(z_1|i) \left[\int_0^{z_1} f_{Z_m}(z_m)\, dz_m \right]^{M-1} dz_1 \tag{8}$$

for all $m \neq 1$

since for all $m \neq 1$ the random variables Z_m are identical and independent. The noise-normalized random variables Z_{mk}, $m = 1, 2, \cdots, M$, are related to the outputs of each demodulator branch by

$$Z_{mk} = \frac{X_{mk}}{\sigma_k^2}, \quad m = 1, 2, \cdots, M \tag{9}$$

where the random variables X_{mk} represent the outputs of the demodulator branches before the noise normalization operation for each hop of a symbol. Let the subscript $n = 1, 2$ denote when hop k of a symbol has interference and has no interference, respectively. The output random variable from the diversity summer for each demodulator branch after combining L independent hops is obtained from

$$\begin{aligned} Z_m &= \sum_{k=1}^{L} Z_{mk_n} \\ &= \sum_{k=1}^{i} Z_{mk_1} + \sum_{k=L-i}^{L} Z_{mk_2}, \quad m = 1, 2, \cdots, M \end{aligned} \tag{10}$$

B. PROBABILITY DENSITY FUNCTION OF THE NARROWBAND INTERFERENCE NOISE POWER

Although the narrowband interference signal for hop k of a symbol is modeled as a Gaussian random variable, it is assumed to be affected by the Rician fading channel. Hence, the amplitude of the narrowband interference signal is modeled as a Ricean random variable, and the probability density function of the narrowband interference noise power is [7]

$$f_{\Sigma_I^2}(\sigma_I^2) = \frac{1}{2\sigma_{\sigma_I}^2} \exp\left(-\frac{\sigma_I^2 + \alpha_{\sigma_I}^2}{2\sigma_{\sigma_I}^2}\right) I_0\left(\frac{\alpha_{\sigma_I}\sqrt{\sigma_I^2}}{\sigma_{\sigma_I}^2}\right) u(\sigma_I^2) \tag{11}$$

where $\alpha_{\sigma_I}^2$ is the average power of the direct component of the narrowband interference signal and $2\sigma_{\sigma_I}^2$ is the average power of the diffuse component of the narrowband interference signal. The ratio of the direct to the diffuse component of the narrowband interference signal is $\alpha_{\sigma_I}^2 / 2\sigma_{\sigma_I}^2 = R2$. The total average received narrowband

interference signal power, $\overline{\sigma}_I^2 = \alpha_{\sigma_I}^2 + 2\sigma_{\sigma_I}^2$, of hop k of a symbol is assumed to remain constant from hop to hop when it is present. Since the average power received due to thermal noise and other wideband interference is not considered a random variable, the probability density function for the total noise power received with hop k of a symbol when partial-band interference is present is obtained from (11) and the linear transformation of random variables given by (3) as

$$\begin{aligned} f_{\Sigma_k^2}(\sigma_k^2) &= f_{\Sigma_I^2}(\sigma_k^2 = \sigma_k^2 - \sigma_T^2)\left|\frac{d\sigma_I^2}{d\sigma_k^2}\right| \\ &= \frac{1}{2\sigma_{\sigma_I}^2}\exp\left(-\frac{\sigma_k^2 - \sigma_T^2 + \alpha_{\sigma_I}^2}{2\sigma_{\sigma_I}^2}\right) \\ &\quad \times I_0\left(\frac{\alpha_{\sigma_I}\sqrt{\sigma_k^2 - \sigma_T^2}}{\sigma_{\sigma_I}^2}\right) u(\sigma_k^2 - \sigma_T^2) \end{aligned} \tag{12}$$

C. PROBABILITY DENSITY FUNCTION OF THE DECISION VARIABLE Z_m, $m = 2, 3, \cdots, M$

The conditional probability density functions of the identical, independent random variables X_{mk}, $m = 2, 3, \cdots, M$ that represent the signal for hop k of a symbol at the outputs of the quadratic detectors of the demodulator branches that do not contain a signal are [7]

$$f_{X_{mk}}(x_{mk}|\sigma_k^2, i) = \frac{1}{2\sigma_k^2}\exp\left(-\frac{x_{mk}}{2\sigma_k^2}\right) u(x_{mk}), \quad m = 2, 3, \cdots, M \tag{13}$$

where $u(\cdot)$ is the unit step function. The probability density functions of the noise-normalized random variables Z_{mk}, $m = 2, 3, \cdots, M$ are obtained from (13) and the transformation of random variables indicated by (9) as [16]

$$\begin{aligned} f_{Z_{mk}}(z_{mk}) &= \int_{-\infty}^{\infty} \sigma_k^2 f_{X_{mk}}\left(x_{mk} = z_{mk}\sigma_k^2 | \sigma_k^2\right) f_{\Sigma_k^2}(\sigma_k^2) d\sigma_k^2 \\ &= \int_0^{\infty} \frac{\sigma_k^2}{2\sigma_k^2}\exp\left(-\frac{z_{mk}\sigma_k^2}{2\sigma_k^2}\right) u(z_{mk}\sigma_k^2) f_{\Sigma_k^2}(\sigma_k^2) d\sigma_k^2 \\ &= \frac{1}{2}\exp\left(-\frac{z_{mk}}{2}\right) u(z_{mk}) \int_0^{\infty} f_{\Sigma_k^2}(\sigma_k^2) d\sigma_k^2 \end{aligned} \tag{14}$$

$$= \frac{1}{2}\exp\left[-\frac{z_{mk}}{2}\right]u(z_{mk}), \quad m = 2,3,\cdots,M$$

since $u(z_{mk}) = u(z_{mk}\sigma_k^2)$ and $\int_0^\infty f_{\Sigma_k^2}(\sigma_k^2)d\sigma_k^2 = 1$.

The Z_{mk}'s corresponding to demodulator branches with no signal are independent not only of the signal but, due to the normalization used, also of the interference; consequently, for each hop $k = 1,2,\cdots,L$, the noise-normalized random variables that represent the outputs of demodulator branches with no signal present are identical, independent random variables that are independent of channel fading affecting either the signal or the interference. Since each hop is independent, it can be seen from (10) that the Laplace transform of $f_{Z_m}(z_m)$ is

$$F_{Z_m}(s) = [F_{Z_{mk}}(s)]^L \tag{15}$$

where

$$F_{Z_{mk}}(s) = \frac{1}{2(s+1/2)} \tag{16}$$

is the Laplace transform of $f_{Z_{mk}}(z_{mk})$ [17]. Substitution of (16) into (15) yields

$$\begin{aligned} F_{Z_m}(s) &= \left[\frac{1}{2(s+1/2)}\right]^L \\ &= \left(\frac{1}{2}\right)^L \left(\frac{1}{s+1/2}\right)^L \end{aligned} \tag{17}$$

The inverse Laplace transform of (17) is

$$\begin{aligned} f_{Z_m}(z_m) &= \left(\frac{1}{2}\right)^L \frac{z_m^{L-1}}{(L-1)!}\exp\left(-\frac{z_m}{2}\right)u(z_m) \\ &= \frac{(z_m/2)^{L-1}}{2(L-1)!}\exp\left(-\frac{z_m}{2}\right)u(z_m), \quad m = 2,3,\cdots,M \end{aligned} \tag{18}$$

Substitution of (18) into (8) yields [18]

$$P_s(i) = 1 - \int_0^\infty f_{z_1}(z_1|i)\left[\int_0^{z_1}\frac{(z_m/2)^{L-1}}{2(L-1)!}\exp\left(-\frac{z_m}{2}\right)dz_m\right]^{M-1}dz_1 \tag{19}$$

Substitution of $x = z_m/2$ in (19) results in

$$P_s(i) = 1 - \int_0^\infty f_{z_1}(z_1|i) \left[\int_0^{z_1/2} \frac{(x)^{L-1}}{(L-1)!} \exp(-x) dx \right]^{M-1} dz_1 \qquad (20)$$

which can be evaluated to yield

$$\begin{aligned} P_s(i) &= 1 - \int_0^\infty f_{z_1}(z_1|i) \times \left\{ \frac{\exp(-x)}{(L-1)!} \right. \\ &\quad \left. \left[-x^{L-1} + \sum^{L-1} -1(L-1)(L-2)\cdots(L-k)x^{L-1-k} \right] \Big|_0^{z_1/2} \right\}^{M-1} dz_1 \\ &= 1 - \int_0^\infty f_{z_1}(z_1|i) \times \left\{ \frac{\exp\left(-\frac{z_1}{2}\right)}{(L-1)!} \right. \\ &\quad \left. \left[-\left(\frac{z_1}{2}\right)^{L-1} - \sum^{L-1}(L-1)(L-2)\cdots(L-k)\left(\frac{z_1}{2}\right)^{L-1-k} + 1 \right] \right\}^{M-1} dz_1 \\ &= 1 - \int_0^\infty f_{Z_1}(z_1|i) \left[1 - \exp\left(\frac{-z_1}{2}\right) \sum_{k=0}^{L-1} \frac{\left(\frac{z_1}{2}\right)^{L-1-k}}{(L-1-k)!} \right]^{M-1} dz_1 \qquad (21) \end{aligned}$$

As $z_1 \to \infty$, the bracketed term in (21) approaches unity which indicates the integral converges. Use of $\int_0^\infty f_{Z_1}(z_1|i)\, dz_1 = 1$ in (21), yields a more computationally efficient expression

$$P_s(i) = \int_0^\infty f_{Z_1}(z_1|i) \left\{ 1 - \left[1 - \exp\left(\frac{-z_1}{2}\right) \sum_{k=0}^{L-1} \frac{\left(\frac{z_1}{2}\right)^{L-1-k}}{(L-1-k)!} \right]^{M-1} \right\} dz_1 \qquad (22)$$

In order to complete the evaluation of (22), $f_{Z_1}(z_1|i)$ is required. This issue is addressed in the next subsection.

D. PROBABILITY DENSITY FUNCTION OF THE DECISION VARIABLE Z_1

The conditional probability density function of the random variable X_{1k} that represents the detector output of branch 1 of the demodulator, given a signal amplitude $\sqrt{2}\,a_k$, is [7]

$$f_{X_{1k}}(x_{1k}|a_k,\sigma_k^2) = \frac{1}{2\sigma_k^2}\exp\left(-\frac{x_{1k}+2a_k^2}{2\sigma_k^2}\right) I_0\left(\frac{a_k\sqrt{2x_{1k}}}{\sigma_k^2}\right) u(x_{1k}) \qquad (23)$$

where $I_n(\cdot)$ represents the modified Bessel function of the first kind and order n. Fading of the communications signal for hop k of a symbol is modeled by assuming a_k to be a Rician random variable. The probability density function of the Rician random variable a_k is [7]

$$f_{A_k}(a_k) = \frac{a_k}{\sigma^2}\exp\left(-\frac{a_k^2+\alpha^2}{2\sigma^2}\right) I_0\left(\frac{a_k\alpha}{\sigma^2}\right) u(a_k) \qquad (24)$$

where α^2 is the average power of the direct component of the communications signal and $2\sigma^2$ is the average power of the diffuse component of the communications signal. The ratio of the direct to the diffuse component of the communications signal is $\alpha^2/2\sigma^2 = R1$. The average received signal power of hop k of a symbol is assumed to remain constant from hop to hop.

The conditional probability density function of the noise-normalized random variable Z_{1k} is obtained from (23) and the transformation of random variables indicated by (9) as

$$\begin{aligned} f_{Z_{1k}}(z_{1k}|a_k,\sigma_k^2) &= f_{X_{1k}}(x_{1k}=z_{1k}\sigma_k^2|a_k,\sigma_k^2)\left|\frac{dz_{1k}}{dx_{1k}}\right| \\ &= \frac{\sigma_k^2}{2\sigma_k^2}\exp\left(-\frac{z_{1k}\sigma_k^2-2a_k^2}{2\sigma_k^2}\right) I_0\left(\frac{a_k\sqrt{2z_{1k}\sigma_k^2}}{\sigma_k^2}\right) u(z_{1k}\sigma_k^2) \\ &= \frac{1}{2}\exp\left(-\frac{\sigma_k^2 z_{1k}+2a_k^2}{2\sigma_k^2}\right) I_0\left(\frac{a_k\sqrt{2z_{1k}}}{\sigma_k}\right) u(z_{1k}) \qquad (25) \end{aligned}$$

The conditioning of Z_{1k} on a_k is removed by integrating the product (25) and (24) with respect to a_k from 0 to ∞ to obtain [18]

$$f_{Z_{1k}}(z_{1k}|\sigma_k^2) = \int_0^\infty f_{Z_{1k}}(z_{1k}|a_k,\sigma_k^2) f_{A_k}(a_k) da_k \tag{26}$$

$$\begin{aligned} f_{Z_{1k}}(z_{1k}|\sigma_k^2) &= \int_0^\infty \frac{1}{2}\exp\left(-\frac{\sigma_k^2 z_{1k}+2a_k^2}{2\sigma_k^2}\right) \\ &\quad \times I_0\left(\frac{a_k\sqrt{2z_{1k}}}{\sigma_k}\right)\frac{a_k}{\sigma^2}\exp\left(-\frac{a_k^2+\alpha^2}{2\sigma^2}\right) I_0\left(\frac{a_k\alpha}{\sigma^2}\right) da_k \\ &= \frac{1}{2\sigma^2}\exp\left(-\frac{z_{1k}2\sigma^2+\alpha_k^2}{2\sigma^2}\right) \\ &\quad \times \int_0^\infty a_k \exp\left(-\frac{a_k^2(2\sigma^2+\sigma_k^2)}{2\sigma^2\sigma_k^2}\right) I_0\left(\frac{a_k\sqrt{2z_{1k}}}{\sigma_k}\right) I_0\left(\frac{a_k\alpha}{\sigma^2}\right) da_k \\ &= \frac{1}{2(1+2\sigma^2/\sigma_k^2)}\exp\left[-\frac{1}{2}\left(\frac{z_{1k}+2\alpha^2/\sigma_k^2}{1+2\sigma^2/\sigma_k^2}\right)\right] I_0\left(\frac{\sqrt{2z_{1k}\alpha^2/\sigma_k^2}}{1+2\sigma^2/\sigma_k^2}\right) u(z_{1k}) \end{aligned} \tag{27}$$

where α^2/σ_k^2 and $2\sigma^2/\sigma_k^2$ are the signal-to-noise ratios of the direct signal component and the diffuse signal component, respectively, of hop k of a symbol.

Let Z_{1k_1} and Z_{1k_2} denote the random variable Z_{1k} when hop k of a symbol has interference and no interference, respectively. Analogously, let $f_{Z_{1k_n}}(z_{1k_n})$, $n = 1,2$ denote the corresponding probability density functions and $\sigma_{k_n}^2$, $n = 1,2$ represent the corresponding noise power when hop k of a symbol has interference and no interference, respectively. Since each hop is independent, it can be seen from (10) that the Laplace transform of $f_{Z_1}(z_1|\sigma_{k_1}^2)$ is

$$F_{Z_1}(s|\sigma_{k_1}^2, i) = \left[F_{Z_{1k_1}}(s|\sigma_{k_1}^2)\right]^i \left[F_{Z_{1k_2}}(s|\sigma_{k_2}^2)\right]^{L-i} \tag{28}$$

where $\sigma_{k_2}^2$ is not a random variable. The Laplace transform of $f_{Z_{1k_n}}(z_{1k_n}|\sigma_{k_n}^2)$, $n = 1,2$ is [19]

$$F_{Z_{1k_n}}(s|\sigma_{k_n}^2) = \int_0^\infty f_{Z_1}(z_1|\sigma_k^2)\exp(-sz_{1k_n})dz_{1k_n}$$

$$= \int_0^\infty \beta_{k_n} \exp\left[-\beta_{k_n}\left(Z_{1k_n} + \frac{2\alpha^2}{\sigma_k^2}\right)\right]$$
$$\times I_0\left(2\beta_{k_n}\sqrt{2z_{1k}\alpha^2/\sigma_k^2}\right)\exp(-sz_{1k_n})dz_{1k_n}$$
$$= \beta_{k_n}\exp(-2\beta_{k_n}\rho_k)\int_0^\infty \exp\left[-z_{1k_n}(s+\beta_{k_n})\right] I_0\left(2\beta_{k_n}\sqrt{2z_{1k}\rho_k}\right) dz_{1k_n}$$
$$= \frac{\beta_{k_n}}{s+\beta_{k_n}}\exp\left[\frac{-2\rho_k\beta_{k_n}s}{s+\beta_{k_n}}\right] \tag{29}$$

where

$$\beta_{k_n} = \frac{1}{2\left(1+2\sigma^2/\sigma_{k_n}^2\right)} \tag{30}$$

$$\xi_k = \frac{2\sigma^2}{\sigma_{k_n}^2} \tag{31}$$

$$\rho_k = \frac{\alpha^2}{\sigma_k^2} \tag{32}$$

The inverse Laplace transform of (29) raised to the c_n power is [20]

$$\left[f_{Z_{1k_n}}(z_{1k_n}|\sigma_{k_n}^2)\right]^{\circledast c_n} = \mathcal{L}^{-1}\left\{\left[F_{Z_{1k_n}}(s|\sigma_{kn}^2)\right]^{c_n}\right\}$$
$$= \mathcal{L}^{-1}\left\{\left(\frac{\beta_{k_n}}{s+\beta_{k_n}}\right)^{c_n}\exp\left[\frac{-2\rho_k\beta_{k_n}sc_n}{s+\beta_{k_n}}\right]\right\}$$
$$= \beta_{k_n}^{c_n}\mathcal{L}^{-1}\left\{\left(\frac{1}{s+\beta_{k_n}}\right)\exp\left[\frac{-2\rho_k\beta_{k_n}c_n(s+\beta_{k_n})}{s+\beta_{k_n}}\right]\right.$$
$$\left.\times\exp\left(\frac{-2\rho_k\beta_{k_n}^2c_n}{s+\beta_{k_n}}\right)\right\}$$
$$= \beta_{k_n}^{c_n}\exp\left[-2\rho_k\beta_{k_n}c_n\right]\exp\left(-\beta_{k_n}Z_{1k_n}\right)$$
$$\times\mathcal{L}^{-1}\left\{\left(\frac{1}{s}\right)^{c_n}\exp\left[\frac{-2\rho_k\beta_{k_n}^2sc_n}{s}\right]\right\}$$
$$= \beta_{k_n}\left(\frac{z_{1k_n}}{2c_n\rho_k}\right)^{(c_n-1)/2}\exp\left[-\beta_{k_n}(z_{1k_n}+2c_n\rho_k)\right]$$
$$\times I_{c_n-1}\left(2\beta_{k_n}\sqrt{2c_n\rho_kz_{1k_n}}\right)u(z_{1k_n}) \tag{33}$$

where $\otimes c_n$ represents a c_n-fold convolution, $c_1 = i$, and $c_2 = L - i$. Thus,

$$f_{Z_1}\left(z_1|\sigma_k^2, i\right) = \left[f_{Z_{1k_1}}\left(z_1|\sigma_{k_1}^2\right)\right]^{\otimes i} \otimes \left[f_{Z_{1k_2}}(z_{1k_2})\right]^{\otimes L-i} \tag{34}$$

In order to remove the conditioning on the random variable $\sigma_{k_1}^2$ from either (29) or (34), it is necessary to multiply these equations by (12) and integrate the products over the entire range of $\sigma_{k_1}^2$. This is done numerically as required. Since $\sigma_{k_2}^2$ is not a random variable, no further integration is necessary.

III. NUMERICAL RESULTS

A. NUMERICAL PROCEDURE

Computation of the probability of bit error requires the evaluation of (8) for each of the possible combinations of jammed and unjammed hops given L hops per symbol. For the special case of all hops free of interference, σ_k^2 is not a random variable, and the probability density function of Z_1 is given by (33) with $c_n = L$ and $n = 2$. In this case, (8) can be evaluated analytically [21], but the result is so complex that it is easier and more straightforward to evaluate (8) numerically. For the special case of all hops jammed, the conditional probability density function of Z_1 is given by (33) with $c_n = L$ and $n = 1$. The conditioning on $\sigma_{k_1}^2$ is removed numerically as discussed at the end of the last section, and (8) is evaluated numerically. When i hops of a symbol have interference $f_{Z_1}(z_1|i)$ must be evaluated numerically. The conditioning on $\sigma_{k_1}^2$ is removed from the Laplace transform of $f_{Z_1}(z_1|\sigma_{k_1}^2, i)$, given by (34), numerically as discussed at the end of the last section, and $f_{Z_1}(z_1|i)$ is obtained by a numerical inversion of $F_{Z_1}(s|i)$ [22]. As in the previous two cases, (8) is then evaluated numerically.

In many cases an analytical solution can be obtained by making the assumptions that $\sigma_I^2 \gg \sigma_T^2$ and $E_b/N_o \gg 1$ [5]. For the system investigated in this thesis, these assumptions do not result in either an analytical solution or any significant simplification. Thus, in this thesis the system is evaluated without making the above assumptions.

B. PERFORMANCE

To obtain worst-case partial-band jamming, the jamming fraction γ which maximizes the probability of bit error is found for various values of diversity, fading

conditions, signal-to-noise power density ratios, and order of modulation. When $L > 2$ or $R1 \leq 1$, the worst case γ is approximately one. Thus, $\gamma = 1$ is used to approximate the worst-case performance curves for $L > 2$ or $R1 \leq 1$. All results presented in this thesis are obtained by assuming that the ratio of direct-to-diffuse signal power $R1$ and the direct-to-diffuse narrowband signal power $R2$ are the same for each hop k of a symbol.

Receiver performance for a signal experiencing Rayleigh fading with slow hopping ($L = 1$) and $M = 2$ is illustrated in Fig. 5 for $E_b/N_0 = 20$ dB. Plots are shown for the narrowband interference experiencing no fading, Rayleigh fading, and Rician fading (specifically, $R2 = 10$), and for both broadband interference ($\gamma = 1$) and partial-band interference ($\gamma = 0.1$). As with the conventional case of no fading of the narrowband interference, worst-case performance is obtained for both Rayleigh fading and Rician fading of the narrowband interference when $\gamma = 1$; that is, partial-band interference has no adverse effect on receiver performance when the signal experiences Rayleigh fading irrespective of the fading experienced by the narrowband interference. As can be seen, there is only a slight improvement in receiver performance when the narrowband interference experiences Rayleigh fading. The signal-to-thermal noise power ratio does not influence the relative effect of fading of the narrowband interference signal on receiver performance.

Receiver performance when there is no signal fading for slow hopping ($L = 1$) and $M = 2$ is illustrated in Figs. 6 and 7 for $E_b/N_0 = 16$ dB. Plots are shown for the narrowband interference experiencing no fading, Rayleigh fading, and Rician fading ($R2 = 10$) for pseudo worst-case partial-band interference where $\gamma = 2/(E_b/N_I)$ [5] in Fig. 6 and broadband interference in Fig. 7. As can be seen, there is very little effect on worst-case receiver performance as a consequence of fading of the narrowband interference. For fixed γ, the counter-intuitive result of poorer receiver

performance when the narrowband interference experiences fading is obtained for a broad range of both the ratio of signal-to-narrowband interference power, E_b/N_I, and γ. This effect is most pronounced for Rayleigh fading.

Receiver performance for a signal experiencing Rician fading ($R1 = 10$) with slow hopping ($L = 1$) and $M = 2$ is illustrated in Fig. 8 for $E_b/N_0 = 16$ dB. Plots are shown for the narrowband interference experiencing no fading, Rayleigh fading, and Rician fading ($R2 = 10$) for pseudo worst-case partial-band interference where $\gamma = 2/(E_b/N_I)$. As in the previous case, there is very little effect on worst-case receiver performance as a consequence of fading of the narrowband interference. Also, as in the previous case, for fixed γ the counter-intuitive result of poorer receiver performance when the narrowband interference experiences fading is obtained for some signal-to-narrowband interference power ratios and for a broad range of γ; although, the effect is much less pronounced and occurs for a much smaller range of E_b/N_I than when the signal does not experience fading.

When the communications signal experiences fading, the probability of bit error, P_b, is increased due to the phase differences of the received signal components. Likewise, when the interference signal experiences fading, the received interference signal components have phase differences. This causes a change in the shape of the noise variance probability density function. The P_b is reduced if the average noise variance, $\overline{\sigma}_k^2$, decreases or if the noise variance probability density function is of a shape to cause the reduction. Since $\overline{\sigma}_k^2$ is held constant in this analysis, then any change in P_b is due to a change in shape of the noise variance probability density function. Without fading of the interference signal, the noise variance probability density function is a delta function, and its effects on P_b are predictable. With fading, the noise variance probability density function is a noncentral Chi-Squared distribution, and its effects on P_b are not predictable.

Since the P_b is proportional to $\exp(-1/2\sigma_k^2)$, then the P_b increases as σ_k^2 increases. In order for the P_b to increase as E_b/N_I increases, the probability density function for the narrowband interference power must weight larger values of σ_k^2 more at large values of E_b/N_I's than lower values of E_b/N_I. The probability density function for Z_1 is the only parameter that depends on the noise power. Therefore, $f_{Z_1}(z_1|\sigma_k^2, i)\, f_{\Sigma_k^2}(\sigma_k^2)$ verses σ_k^2 is plotted in Figs. 9 and 10 illustrating the effect of different direct to diffuse interference power ratios for E_b/N_I's of 0 dB and 10 dB, respectively. In both figures $M = 4$, $E_b/N_0 = 13.35$ dB, $L = 1$, and the three cases where there is essentially no interference fading ($R2 = 100$), Rician fading ($R2 = 10$), and Rayleigh fading ($R2 = 0$) are shown. As can be seen in Fig. 9, the $R2 = 0$ curve is more heavily weighted by the smaller values of σ_k^2. The $R2 = 100$ curve is more heavily weighted by the larger values of σ_k^2. This results in better receiver performance as interference fading increases for $E_b/N_I = 0$. The reverse is observed in Fig. 10 where $E_b/N_I = 10$, thus explaining the results shown in Fig. 7.

Receiver performance with a relatively strong direct signal component ($R1 = 10$), a relatively weak direct interference signal component ($R2 = 1$), and specific partial-band interference fractions are compared to pseudo worst-case performance in Figs. 11–14 for $M = 4$ and diversities of $L = 1, 2, 3$, and 4, respectively. The ratio of bit energy-to-thermal noise density in each of these figures is $E_b/N_0 = 13.35$ dB. The pseudo worst-case partial-band interference for $L = 1$ shown in Fig. 11 is approximated by selecting $\gamma = 2.43/2(E_b/N_I)$ [5]. Partial-band jamming progressively becomes less effective at degrading receiver performance as diversity increases. A composite curve for $L = 2$ is shown in Fig. 12. For $L > 2$, the worst-case γ is approximately unity as can be seen in Figs. 13 and 14. As observed in the case of no interference signal fading [13] and seen in Fig. 11, receiver performance

is degraded more by partial-band interference than by broadband interference when no diversity is used and the E_b/N_I is between about 7 dB to 36 dB.

It is interesting to note by comparing Figs. 11–14 in this thesis with Figs. 2–5 in [13] that the effect of a Rayleigh faded interference signal on receiver performance is slight. The range of E_b/N_I over which partial-band jamming is more effective than barrage jamming is reduced by one dB. Otherwise, the effects are virtually identical. As in Figs. 5–8, there is a very slight difference between receiver performance when the interference signal is not faded and when it experiences Rician fading with $R2 = 10$.

Figures 15–22 illustrate the effects on worst-case receiver performance due to different combinations of effectively Rayleigh (direct/diffuse component =1) and Rician (direct/diffuse component =10) fading for both the communications and interference signals for $L = 4$ and 10, $M = 4$ and 16, and for $E_b/N_0 = 13.35$ and 16 dB. As can be seen in all cases, poorer receiver performance occurs when the interference signal experiences less fading at low E_b/N_I's. At larger values of E_b/N_I's, better receiver performance occurs when the interference signal experiences less fading. When the communications signal has a larger direct component ($R1 = 10$), there is a greater fractional difference between the two curves generated by $R2 = 1$ and $R2 = 10$ than for the case when the communications signal has a small direct component ($R1 = 1$).

A diversity of 10, modulation order of 16, and $E_b/N_0 = 16$ dB are shown in Figs. 15 and 16. The direct signal component is increased from $R1 = 1$ in Fig. 15 to $R1 = 10$ in Fig. 16. There is no effect on the points where the $R2 = 1$ and $R2 = 10$ curves cross at low E_b/N_I's. However, the merge point at larger values of E_b/N_I occur at about 5 dB lower for $R1 = 1$. Also, the receiver's performance is greatly improved by the strong direct component for large values of E_b/N_I.

In Figs. 17 and 18, the ratio of bit energy-to-thermal noise density is reduced to 13.35 dB. Again there is no effect on the points where the $R2 = 1$ and $R2 = 10$ curves cross at low values of E_b/N_I. As E_b/N_0 decreases, the merge point for each curve shifts to a lower value of E_b/N_I. Asymptotic receiver performance significantly decreases as E_b/N_0 decreases. The E_b/N_0 is 16 dB and the modulation order is four in Figs. 19 and 20. The crossover point is again unshifted at low E_b/N_I's, and the merge points of these curves occur at lower values of E_b/N_I as M decreases.

As can be seen by comparing Figs. 15 and 16 to Figs. 21 and 22, respectively, there is a slight increase in receiver performance at low E_b/N_I's, and a great decrease in receiver performance at high E_b/N_I's when diversity is reduced. The increase in receiver performance at low E_b/N_I's is attributed to lower noncoherent combining losses for $L = 4$ than for $L = 10$. It is interesting to note that at low E_b/N_I's, a strong direct component of the interference power has a greater influence in increasing the worst-case receiver performance than a strong direct signal component has in reducing the worst-case receiver performance. The worst-case $P_{b_{R1=1\ R2=10}} > P_{b_{R1=10\ R2=10}} > P_{b_{R1=1\ R2=1}} > P_{b_{R1=10\ R2=1}}$ for low values of E_b/N_I's. This can be seen in Fig. 23 for worst-case receiver performance with $L = 4$, $M = 16$, and $E_b/N_0 = 13.35$ dB. As diversity increases, which is demonstrated in Fig. 24, the worst-case $P_{b_{R1=1\ R2=10}} \approx P_{b_{R1=10\ R2=10}}$ and $P_{b_{R1=1\ R2=1}} \approx P_{b_{R1=10\ R2=1}}$ at low E_b/N_I's.

Worst-case receiver performance for a relatively strong direct signal (R1=10), $E_b/N_0 = 13.35$ dB, diversity of 10, and modulation values of 4, 8, and, 16 are shown in Fig. 25. As can be seen, increased modulation order greatly enhances receiver performance for large values of E_b/N_I. However, it is interesting to note that from about 10 dB to 18 dB, better performance is obtained for $M = 8$ when there is a strong direct interference component ($R2 = 10$) than for $M = 16$ when there is a weak direct interference component ($R2 = 1$). This trend is observed for

the different combinations of diversity, modulation, E_b/N_0, and for a weak direct signal component ($R1 = 1$).

The effects of diversity on worst-case receiver performance are most dramatically displayed in Figs. 26–28. In all three figures, there is a strong direct signal component ($R1 = 100$) and a weak direct interference component ($R2 = 1$). The modulation order is four and $E_b/N_0 = 16$ dB in Fig. 26. Comparison of this figure with Fig. 27, where the modulation order is increased to 16, demonstrates improved receiver performance for a larger range of E_b/N_I's as the modulation value increases. Likewise, comparison of Fig. 27 with Fig. 28, where the modulation order is 16 but E_b/N_0 is reduced to 13.35 dB, shows the significant improvement in receiver performance for a larger range of E_b/N_I's when E_b/N_0 is larger.

The effects on the worst-case receiver performance due to fading of the interference signal is shown in Figs. 29–31. There is a strong direct signal component ($R1 = 10$) and diversities of 3, 6, and 10 in these figures. The modulation order is four in Fig. 29 and 16 in Figs. 30 and 31. The ratio of bit energy-to-thermal noise density is 16 dB in Figs. 29 and 30 and 13.35 dB in Fig. 31. When the direct component of the interference signal is weak ($R2 = 1$) the range of E_b/N_I's where an increase in diversity improves worst-case performance decreases by about 3 dB.

(THIS PAGE INTENTIONALLY LEFT BLANK)

IV. CONCLUSIONS

The effect of fading of the narrowband interference signal on worst-case receiver performance is relatively minor for slow hopping and is more significant for fast hopping. When the signal experiences Rayleigh fading, partial-band interference has no adverse effect on receiver performance irrespective of the fading experienced by the narrowband interference. When there is no signal fading or when the signal fading is Rician and when γ is fixed, the counter-intuitive result of poorer receiver performance when the narrowband interference experiences fading is obtained for some E_b/N_I's for a broad range of γ. The noise variance probability density function is affected by the E_b/N_I in such a manner as to produce counter-intuitive results for a wide range of E_b/N_I's. This effect is most pronounced when the signal does not fade and the narrowband interference signal experiences Rayleigh fading.

Like the noise-normalized receiver without interference fading, partial-band jamming becomes less effective at degrading receiver performance as diversity increases. The receiver performance is also improved at large E_b/N_I's by a strong direct signal component, increasing E_b/N_0, increasing diversity, or larger modulation order. The range of E_b/N_I's where increasing diversity is an advantage is reduced when the interference signal is Rayleigh faded in comparison to the range obtained for a nonfaded interference signal. A Rayleigh faded interference signal with lower modulation order results in better receiver performance than a weakly faded interference signal with a higher modulation order over moderate values of E_b/N_I's. The results obtained for faded interference and nonfaded interference signals asymptotically approach each other at a lower E_b/N_I for weaker direct signals, lower E_b/N_0, lower diversity, or smaller modulation order.

At low E_b/N_I's a strong direct component of the interference power has a greater influence in increasing the worst-case receiver performance than a strong direct signal component has in reducing the worst-case receiver performance. At moderate E_b/N_I values, when the communications signal has a larger direct component, a greater fractional difference between receiver performance exists when the interference signal is Rayleigh faded as compared to when it is weakly faded.

Given the advantage of hindsight, the relatively minor effect that fading of the narrowband interference signal generally has on system performance seems intuitive. Fading is a term used to connote a channel that consists of many different signal paths, that is, multipath, where due to path length differences the various signal components arrive having random phases with respect to one another. When the signal is a standard communications signal, the result is that the various components sometimes combine constructively while other times they add destructively. As a result, the received signal amplitude fluctuates; hence, the term fading. When the signal is noise-like, however, constructive and destructive addition of the multipath signal components has much less effect on the received signal amplitude since the amplitude and phase of the transmitted signal are, in this case, random and rapidly fluctuating to begin with. Thus, channel fading does not significantly affect the received amplitude of a noise-like signal.

The work in this thesis is theoretical. A simulation should be done for comparison. No practical method exists for exact measurement of the average noise power as modeled in the noise-normalized receiver. Hence, further study is needed to investigate receiver performance with the estimated average noise power. The receiver performance against tone jamming was not addressed in this paper. Tone jamming seems likely to be affected more by fading than Gaussian jamming and should be studied.

Previous work has investigated the performance of both the conventional and the noise-normalized noncoherent receiver for constant energy per symbol signaling when communication is corrupted by fading and partial-band interference [10, 11, 12, 13, 23]. However, that work has not considered constant energy per hop signaling. It is unclear whether the noise-normalized noncoherent receiver offers a performance advantage over the conventional noncoherent receiver in the constant energy per hop case, especially when fading is severe. The expense and complexity of the noise-normalized noncoherent receiver may not be justified when utilizing a constant energy per hop system. Since practical military communication systems employ a fixed hop rate and a variable data rate, the constant energy per hop assumption is more logical [24]. Therefore, the most valuable comparison between these two receivers will assume constant energy per hop. This subject should also be addressed.

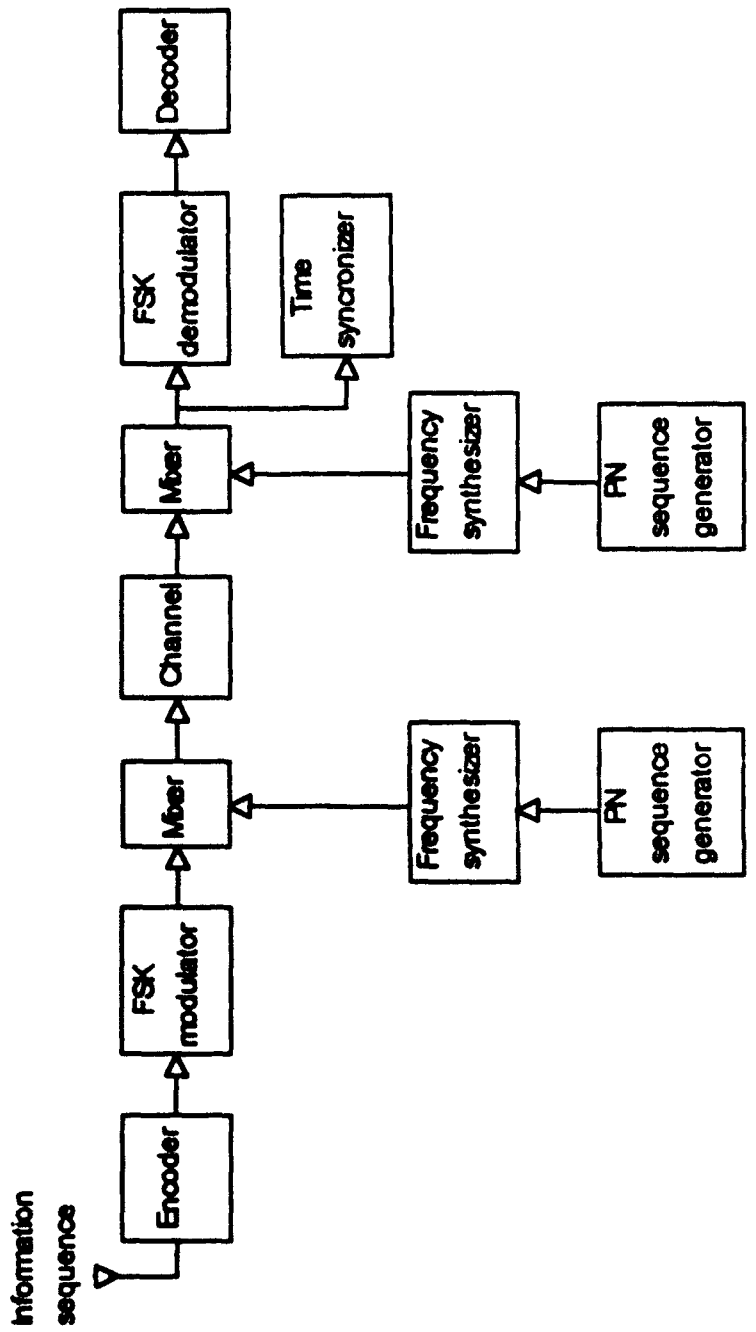

Figure 1. Block diagram of frequency-hopped spread spectrum system.

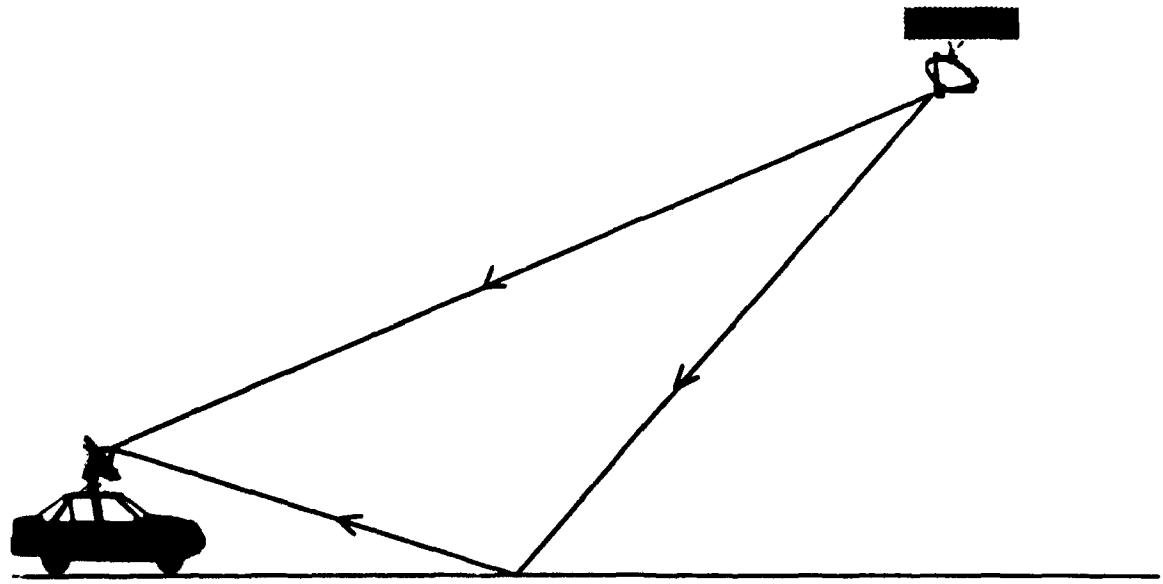

(a)

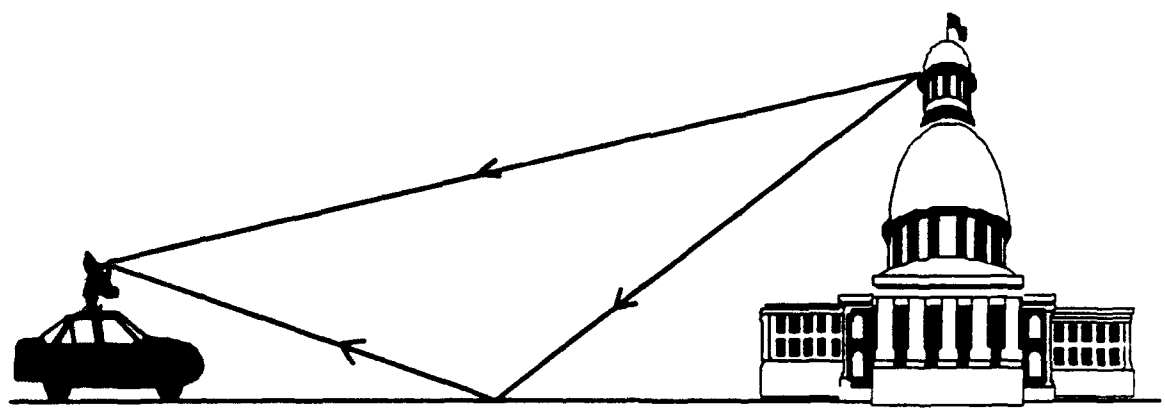

(b)

Figure 2. Multipath progagation for (a) mobile user satellite transmission and (b) mobile user ground transmission.

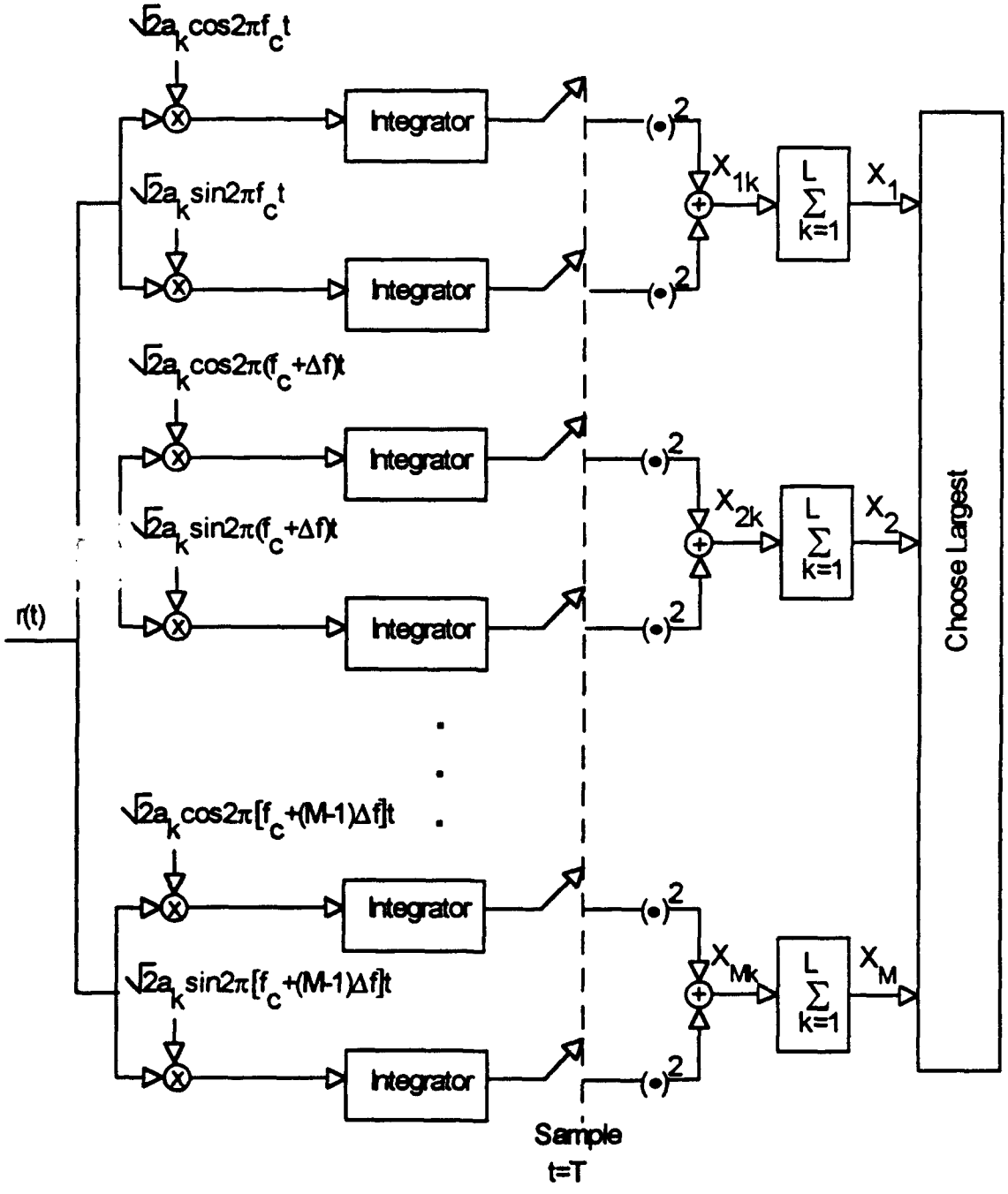

Figure 3. FFH/MFSK conventional noncoherent receiver.

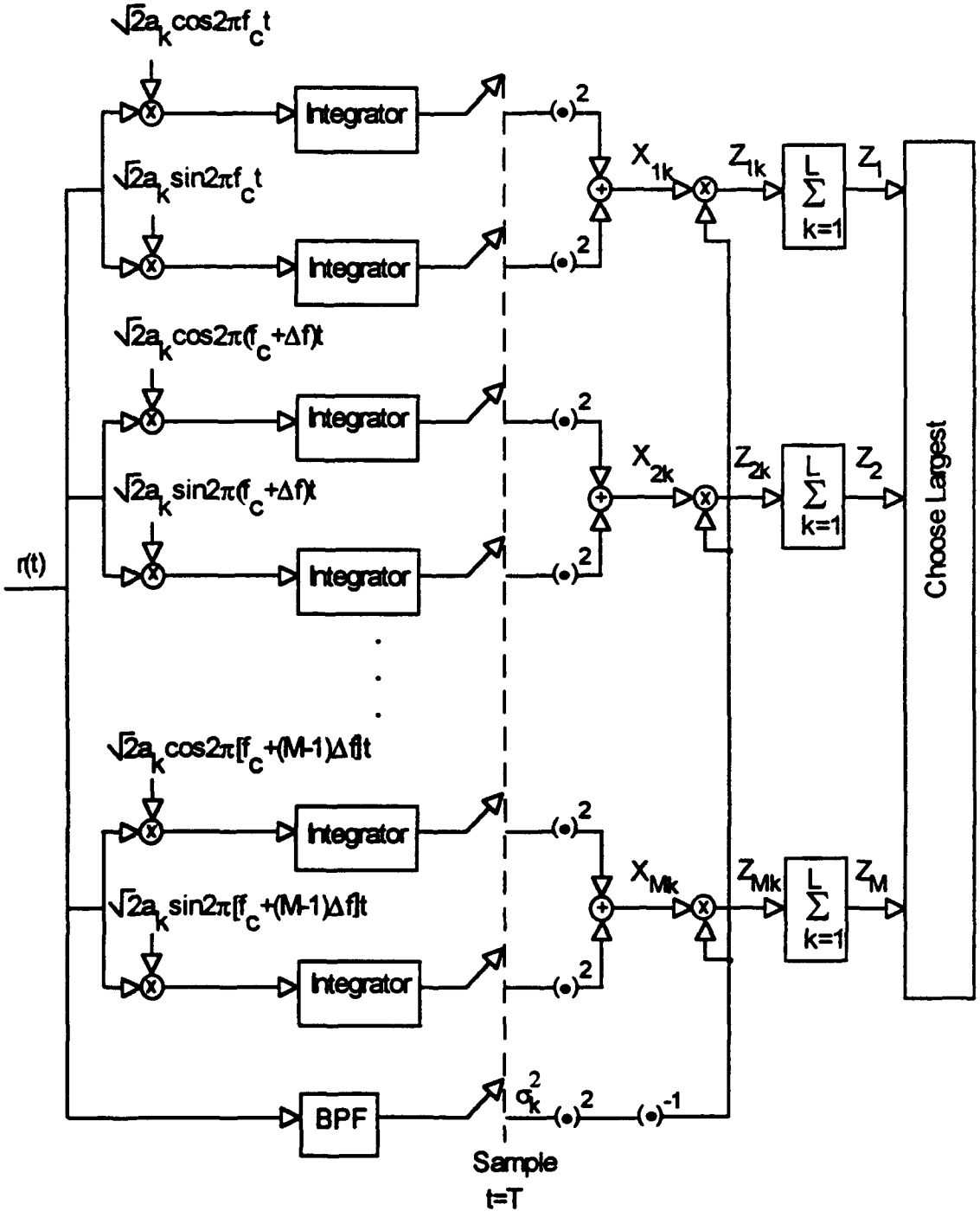

Figure 4. FFH/MFSK noise-normalized receiver.

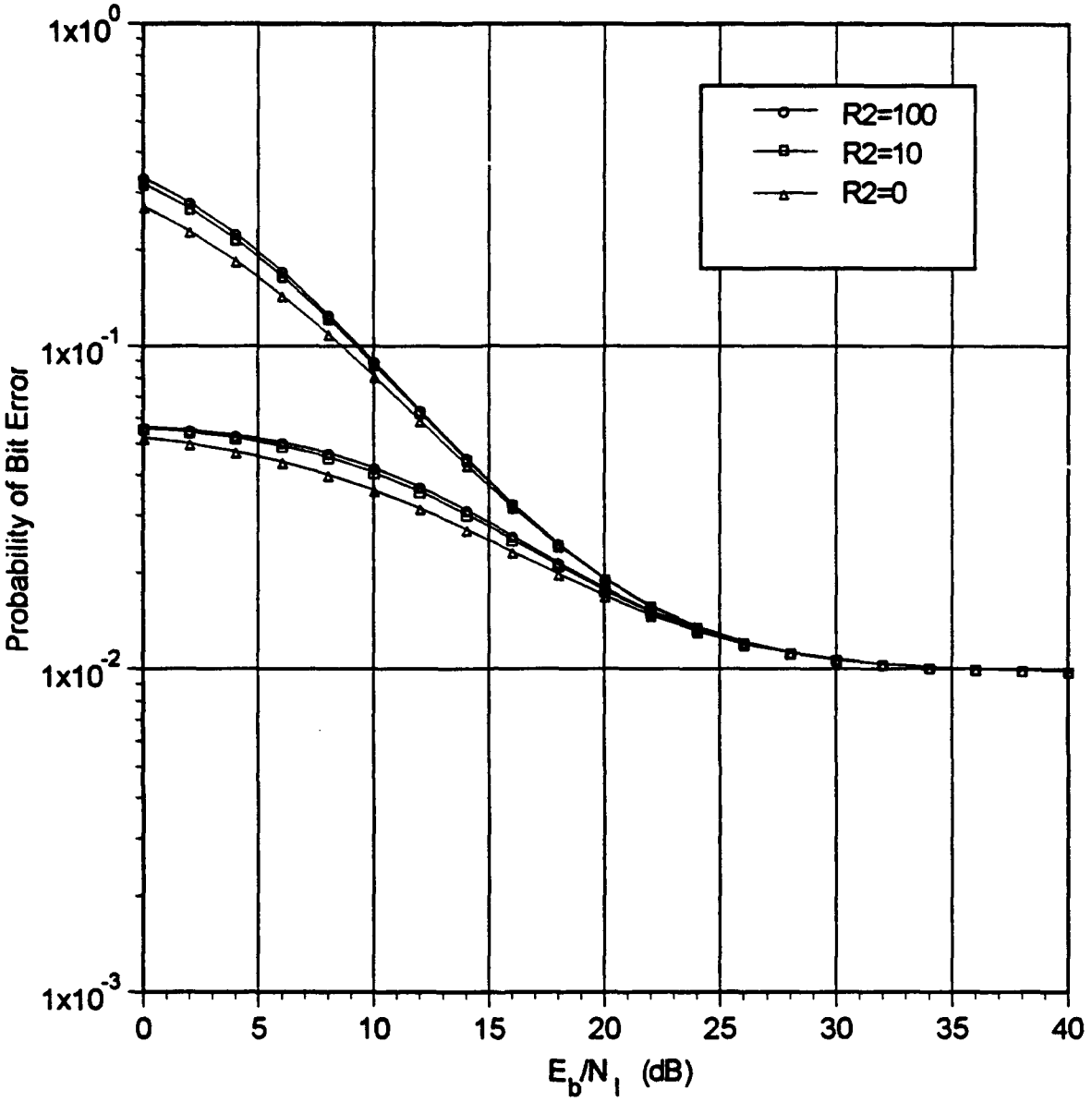

Figure 5. Receiver performance for a Rayleigh faded signal with $L = 1$, $M = 2$, and $E_b/N_0 = 20$ dB. The upper set of curves is obtained with $\gamma = 1$ and the lower set with $\gamma = 0.1$.

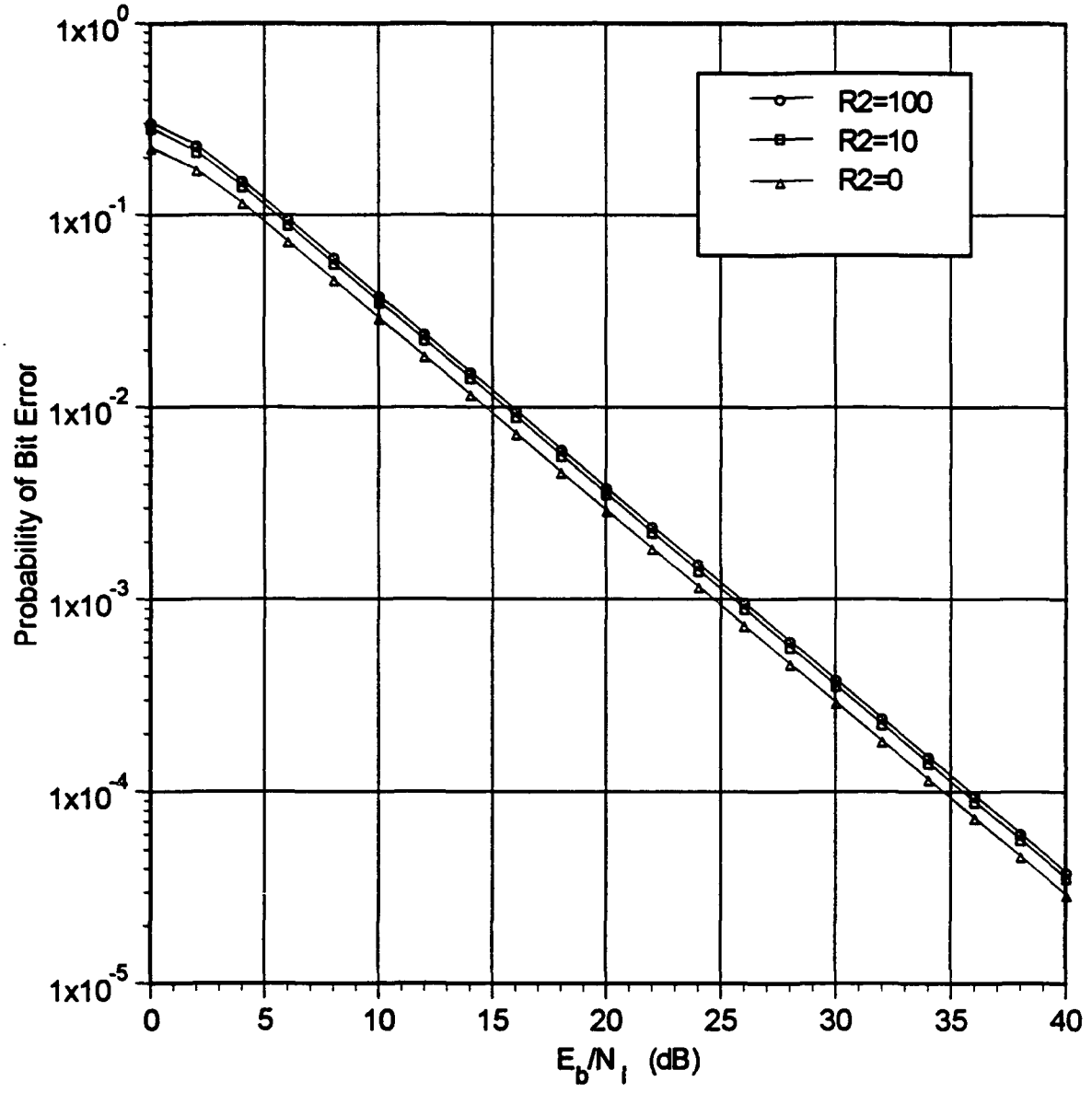

Figure 6. Worst-case receiver performance when there is no signal fading with $L = 1$, $M = 2$, and $E_b/N_0 = 16$ dB.

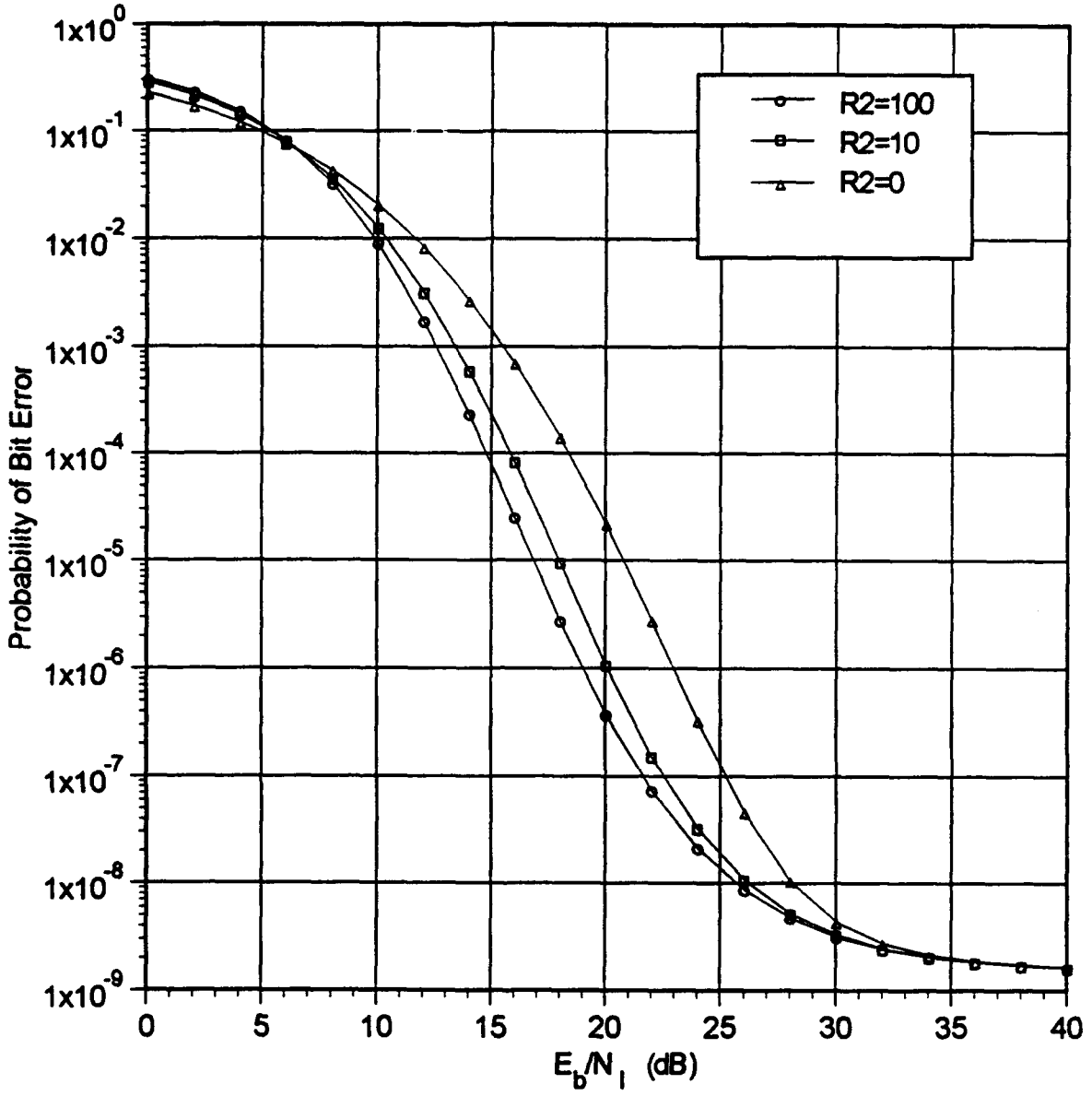

Figure 7. Receiver performance when there is no signal fading with $L = 1$, $M = 2$, $E_b/N_0 = 16$ dB, and $\gamma = 1$.

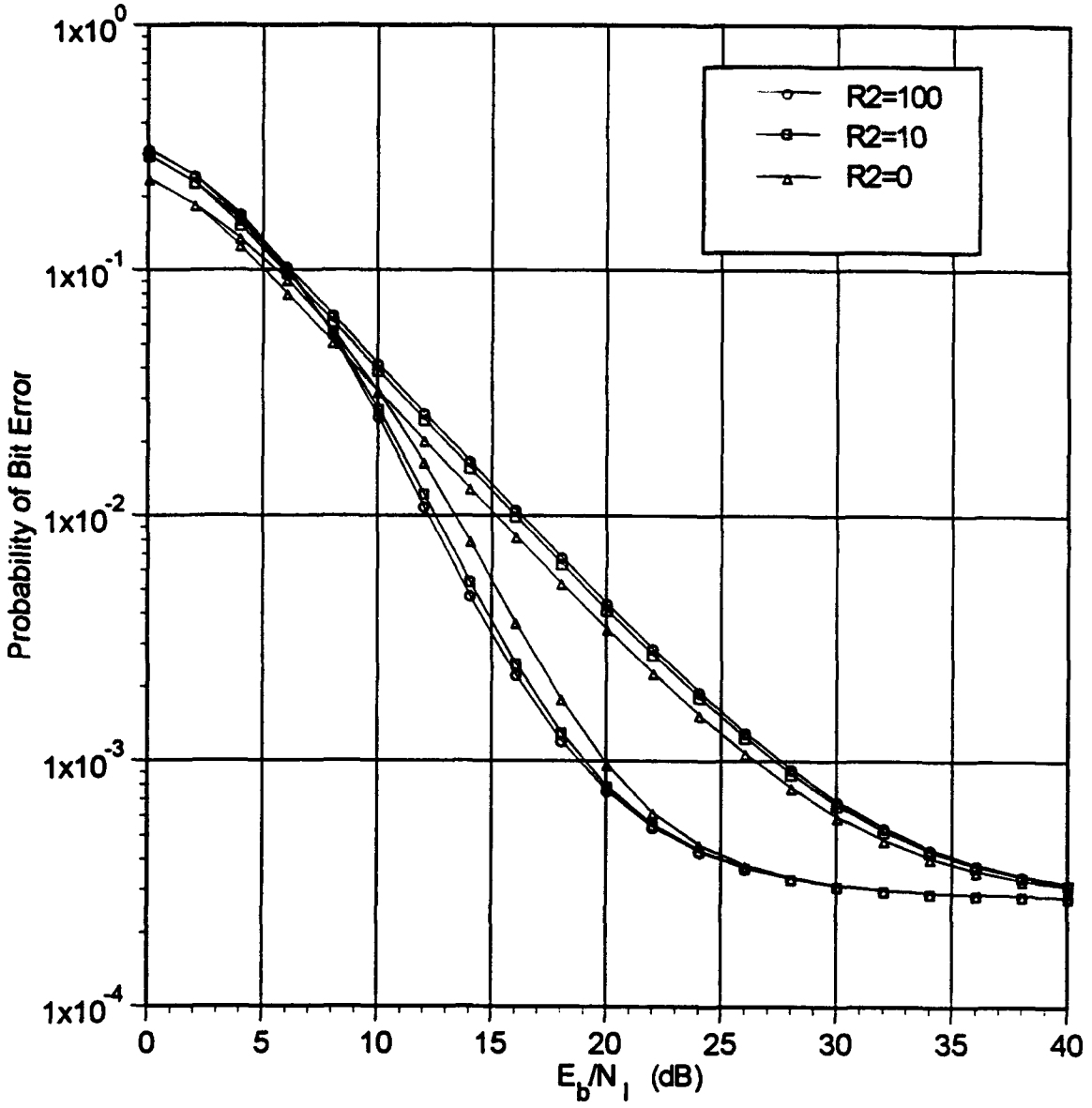

Figure 8. Receiver performance for a Rician faded signal with $L = 1$, $M = 2$, and $E_b/N_0 = 16$ dB. The upper set of curves represent worst-case partial-band interference, while the lower curves are obtained with $\gamma = 1$.

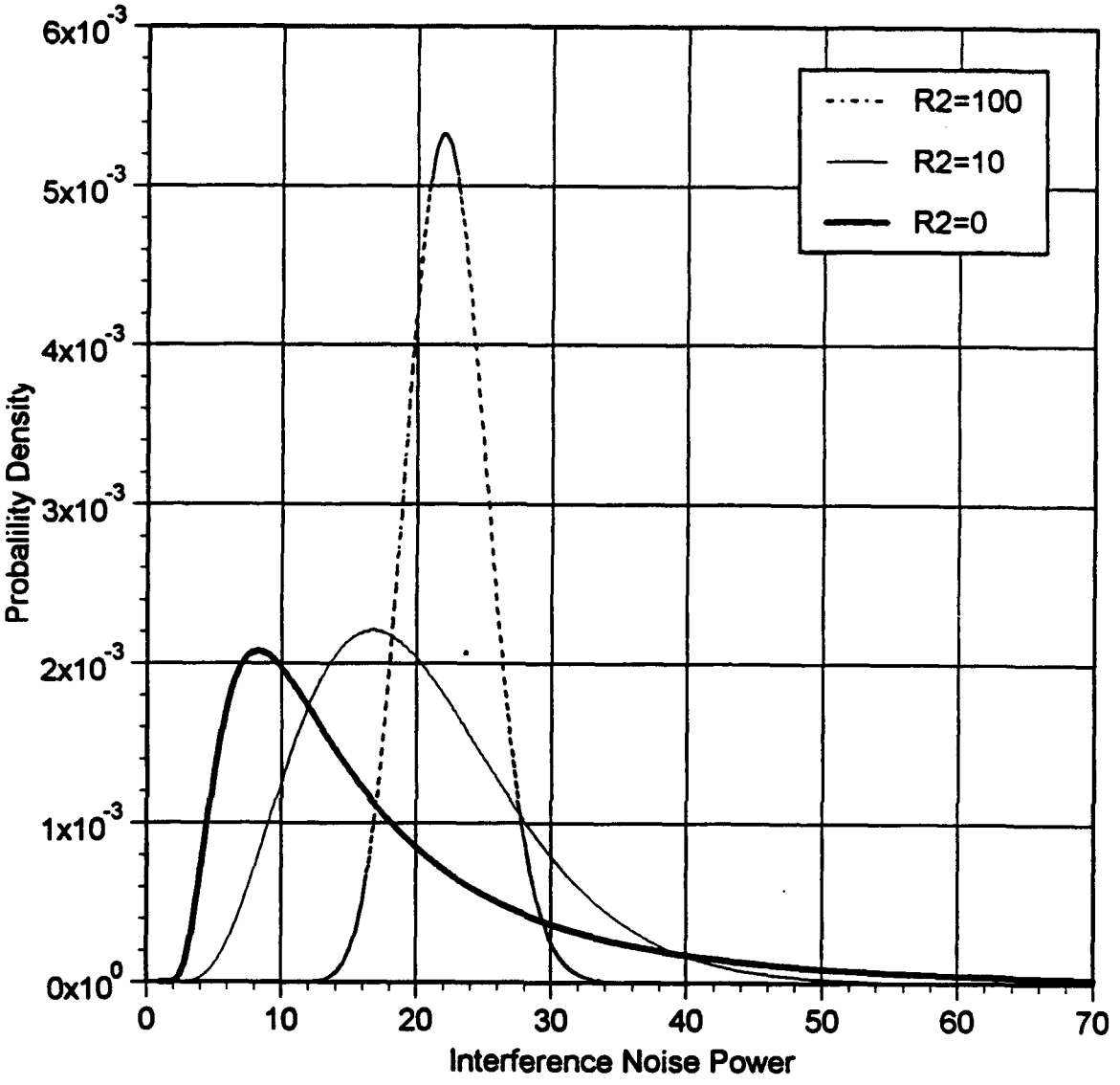

Figure 9. The probability density function for Z_1 conditioned on the noise power multiplied by the noise power probability density function for $z_1 = 5$, $E_b/N_0 = 13.35$ dB, and $E_b/N_I = 0$ dB.

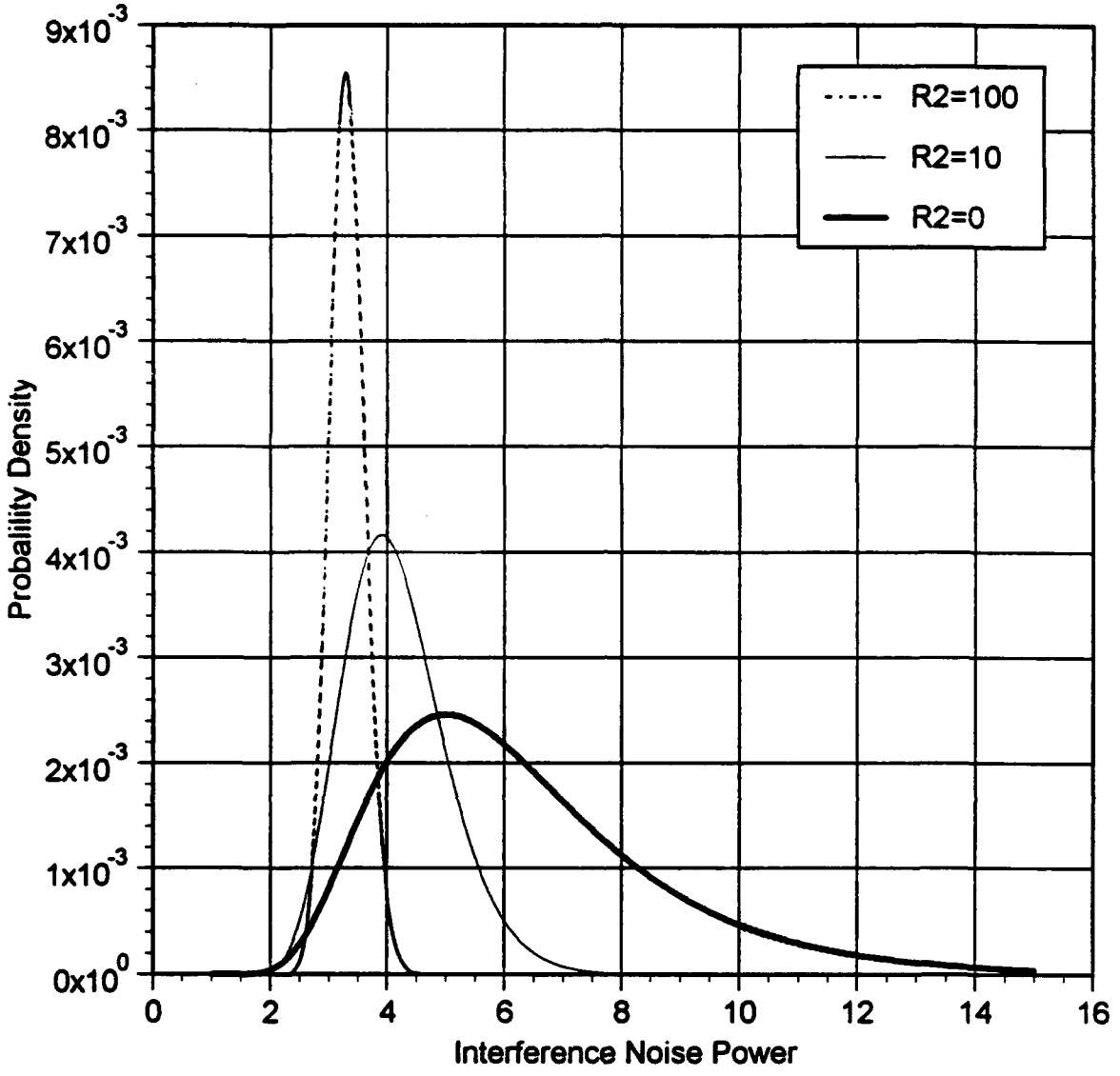

Figure 10. The probability density function for Z_1 conditioned on the noise power multiplied by the noise power probability density function for $z_1 = 5$, $E_b/N_0 = 13.35$ dB, and $E_b/N_I = 10$ dB.

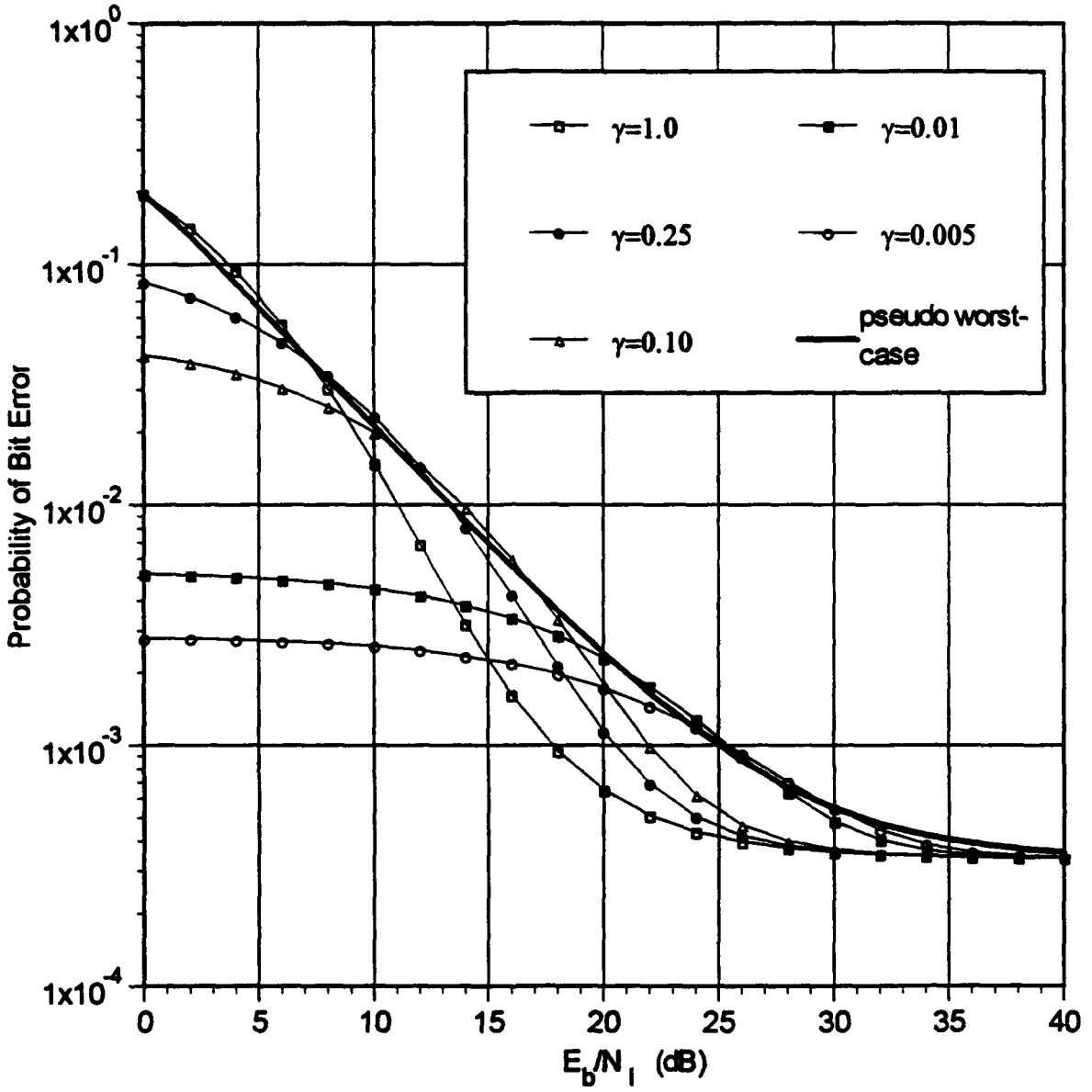

Figure 11. Receiver performance for a Rician faded signal with $L = 1$, $M = 4$, $E_b/N_0 = 13.35$ dB, and partial-band jamming fractions of $\gamma = 1$, 0.25, 0.10, and 0.01 compared to pseudo worst-case performance.

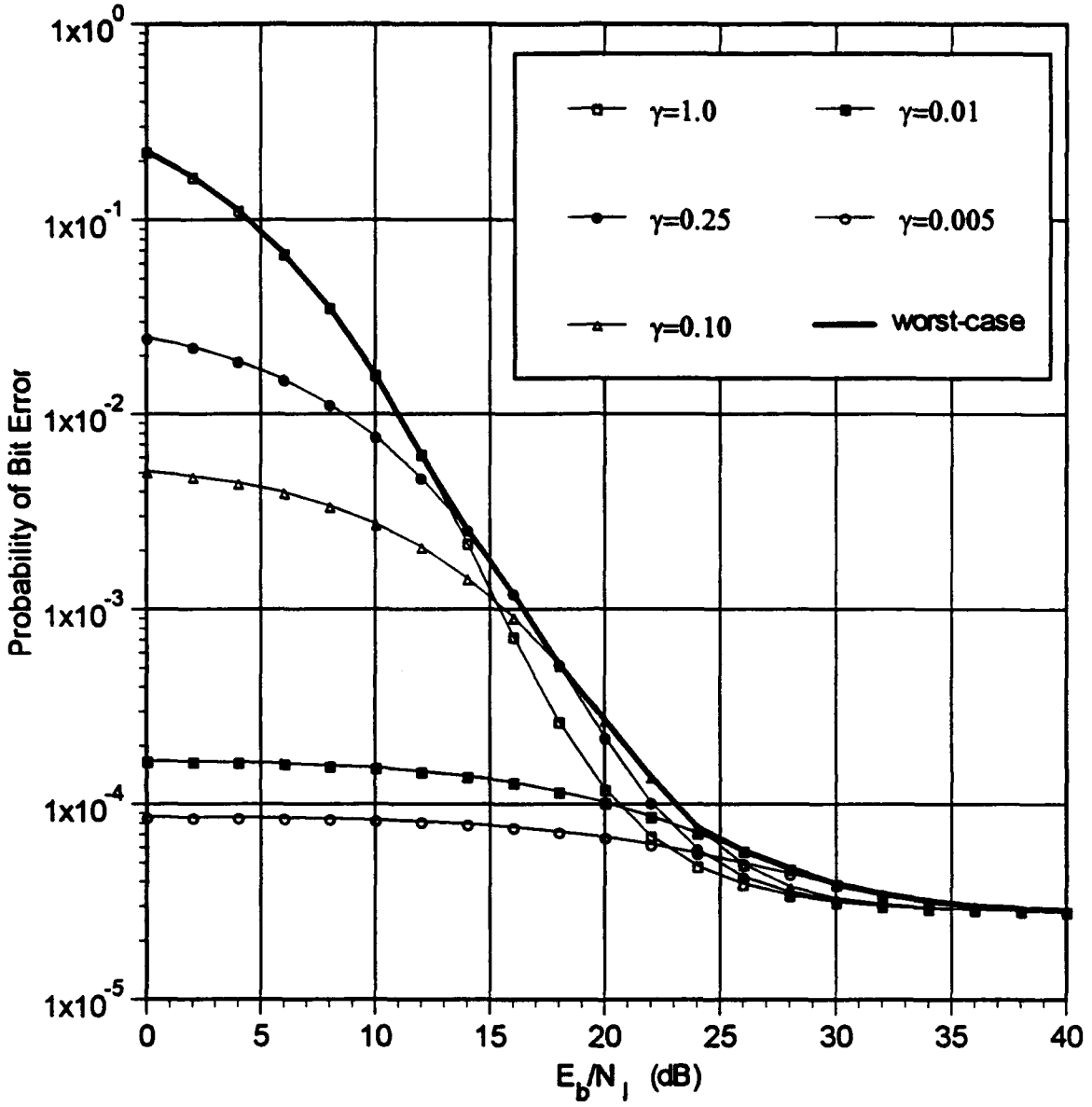

Figure 12. Receiver performance for a Rician faded signal with $L = 2$, $M = 4$, $E_b/N_0 = 13.35$ dB, and partial-band jamming fractions of $\gamma = 1$, 0.25, 0.10, and 0.01 compared to worst-case performance.

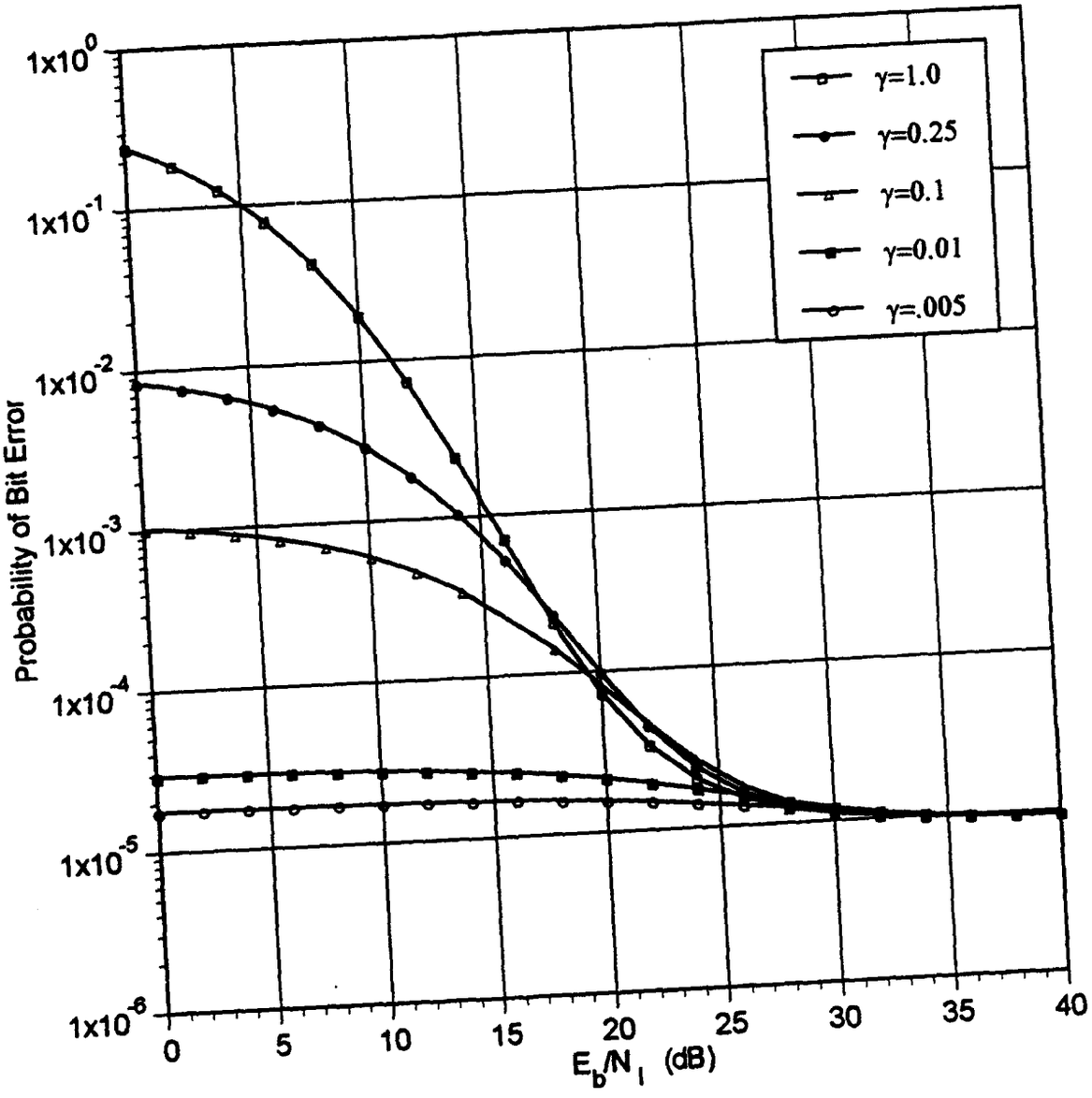

Figure 13. Receiver performance for a Rician faded signal with $L = 3$, $M = 4$, $E_b/N_0 = 13.35$ dB, and partial-band jamming fractions of $\gamma = 1$, 0.25, 0.10, and 0.01 compared to worst-case performance.

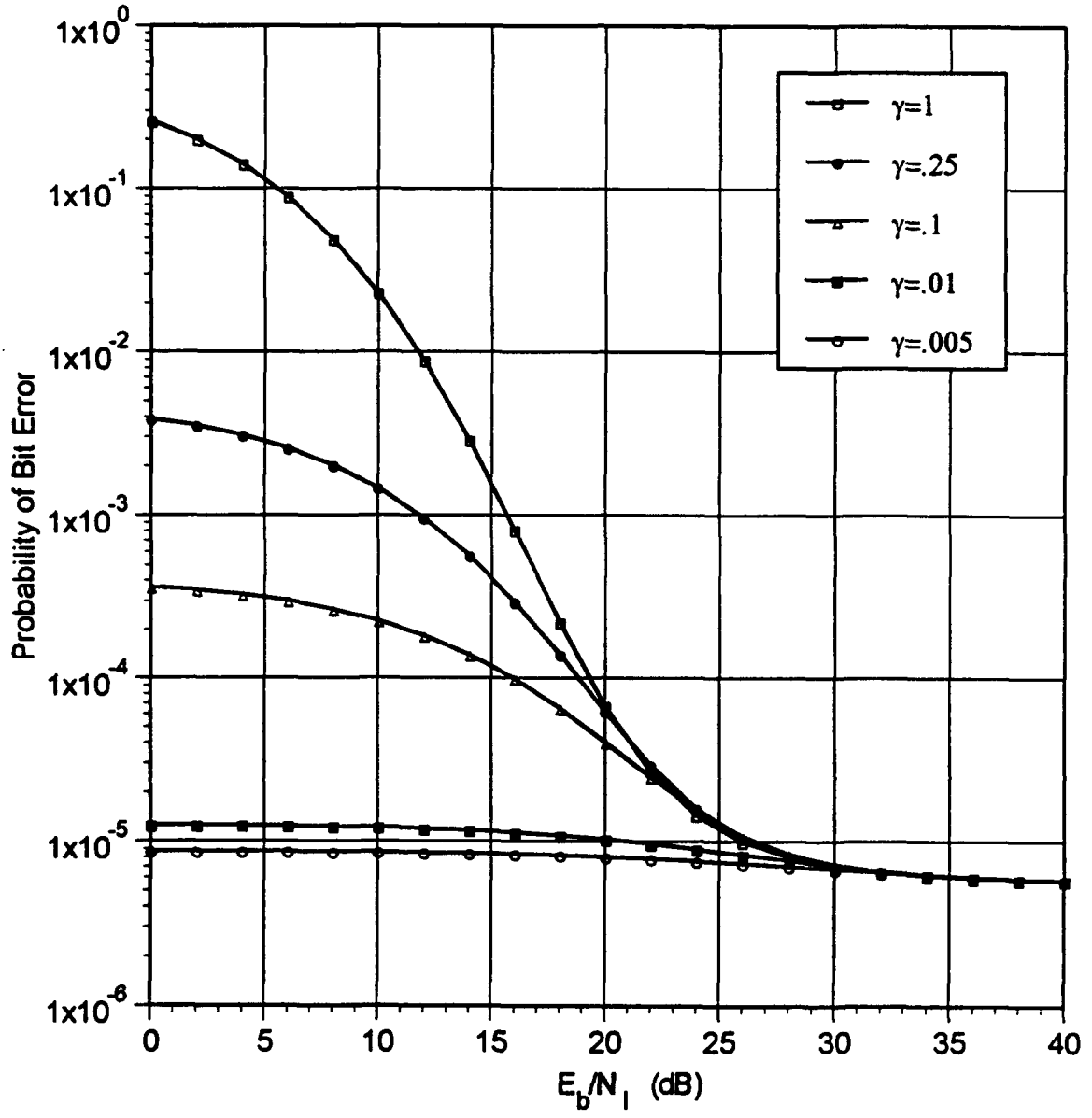

Figure 14. Receiver performance for a Rician faded signal with $L = 4$, $M = 4$, $E_b/N_0 = 13.35$ dB, and partial-band jamming fractions of $\gamma = 1$, 0.25, 0.10, and 0.01 compared to worst-case performance.

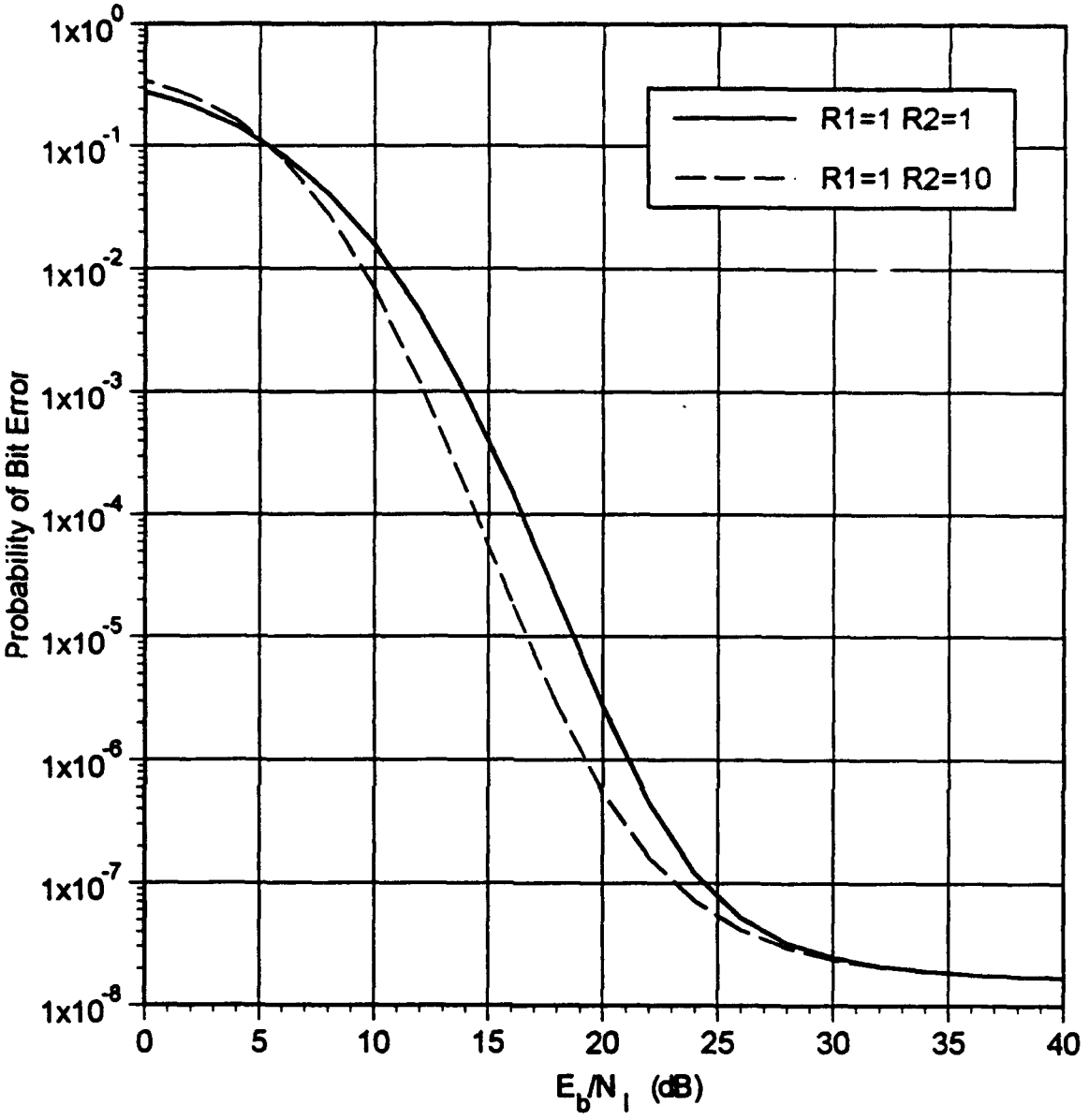

Figure 15. Worst-case receiver performance for a Rayleigh faded signal with Rayleigh and Rician faded interference for $L = 10$, $M = 16$, $E_b/N_0 = 16$ dB.

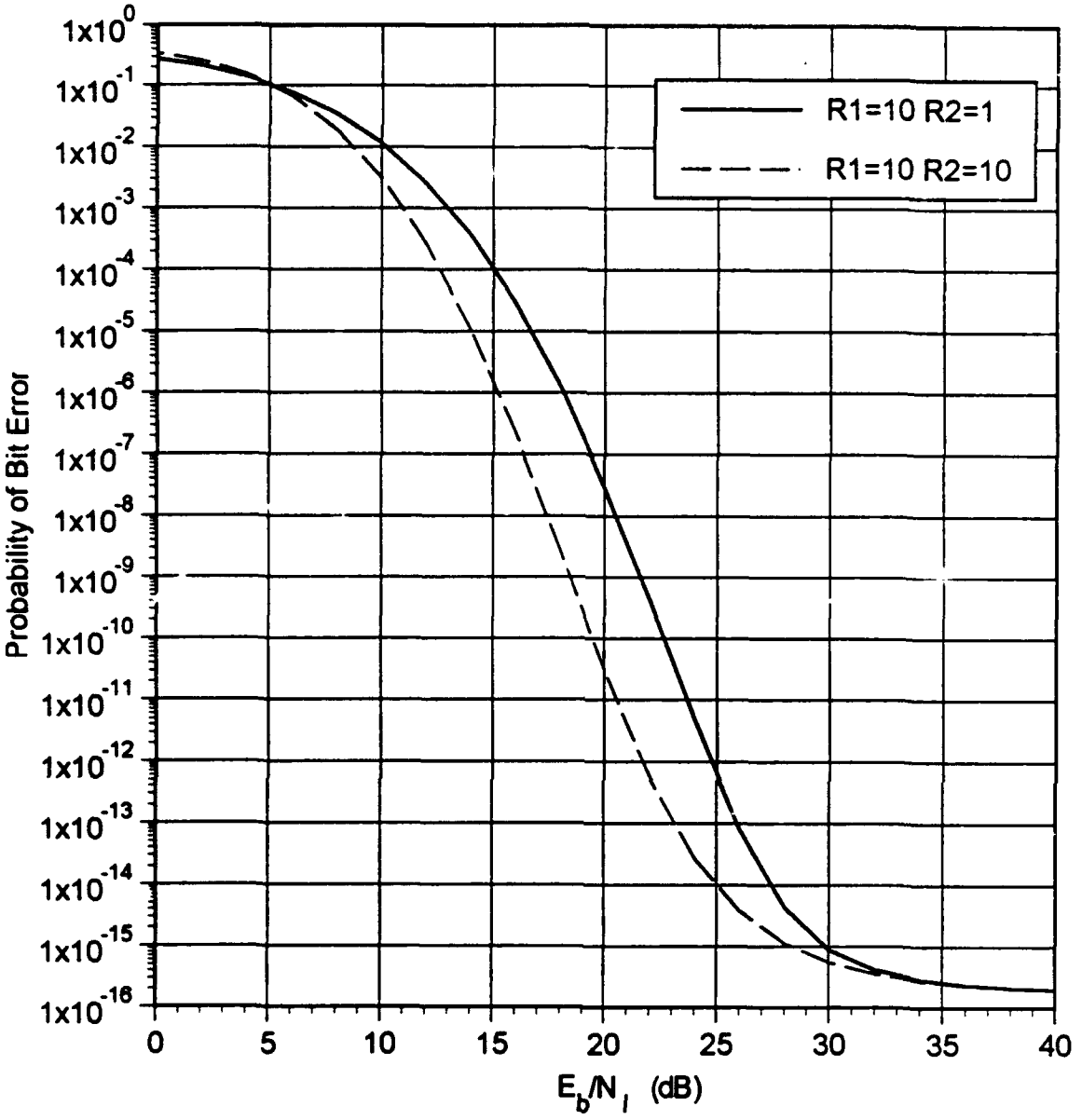

Figure 16. Worst-case receiver performance for a Rician faded signal with Rayleigh and Rician faded interference for $L = 10$, $M = 16$, $E_b/N_0 = 16$ dB.

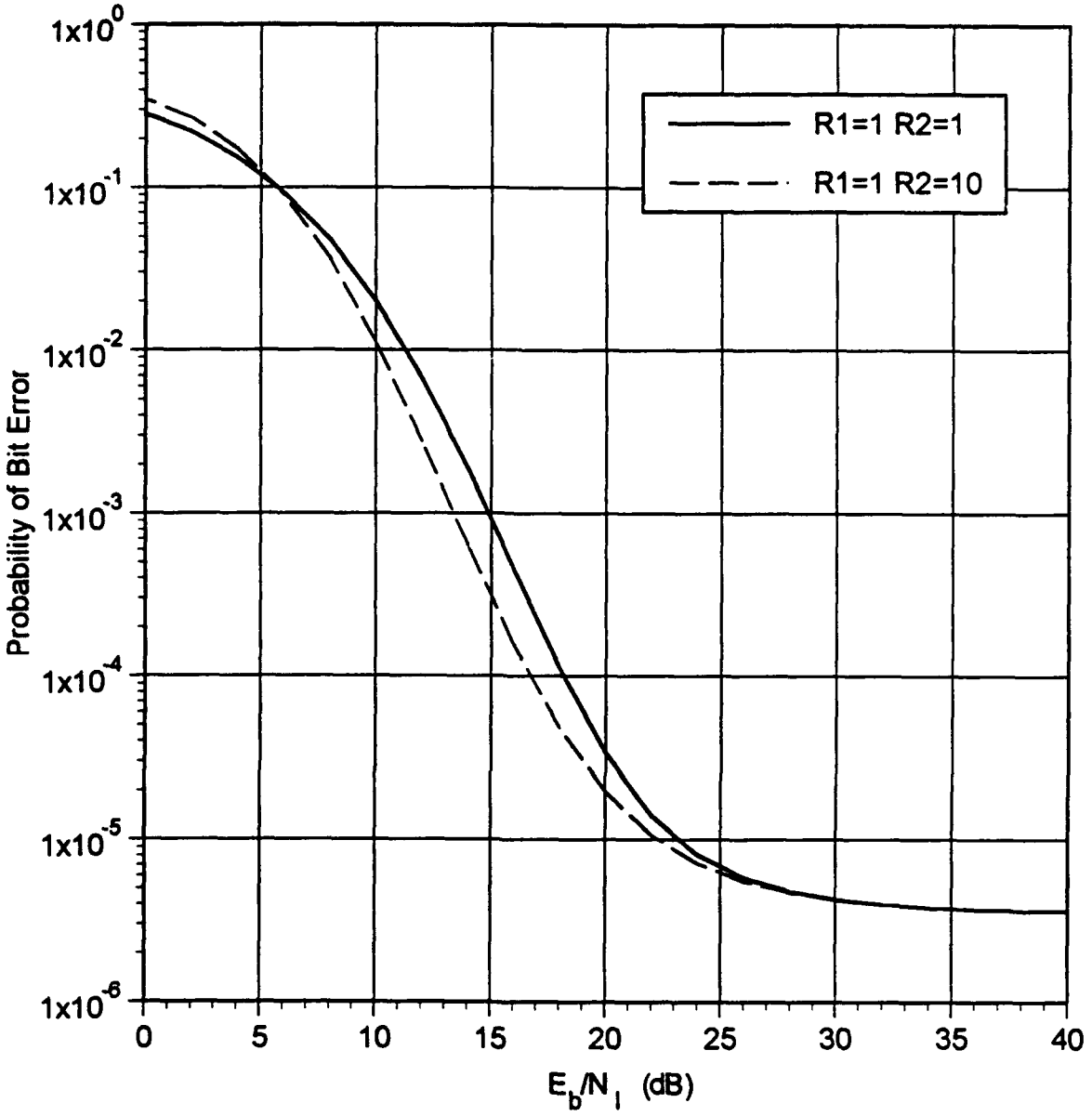

Figure 17. Worst-case receiver performance for a Rayleigh faded signal with Rayleigh and Rician faded interference for $L = 10$, $M = 16$, $E_b/N_0 = 13.35$ dB.

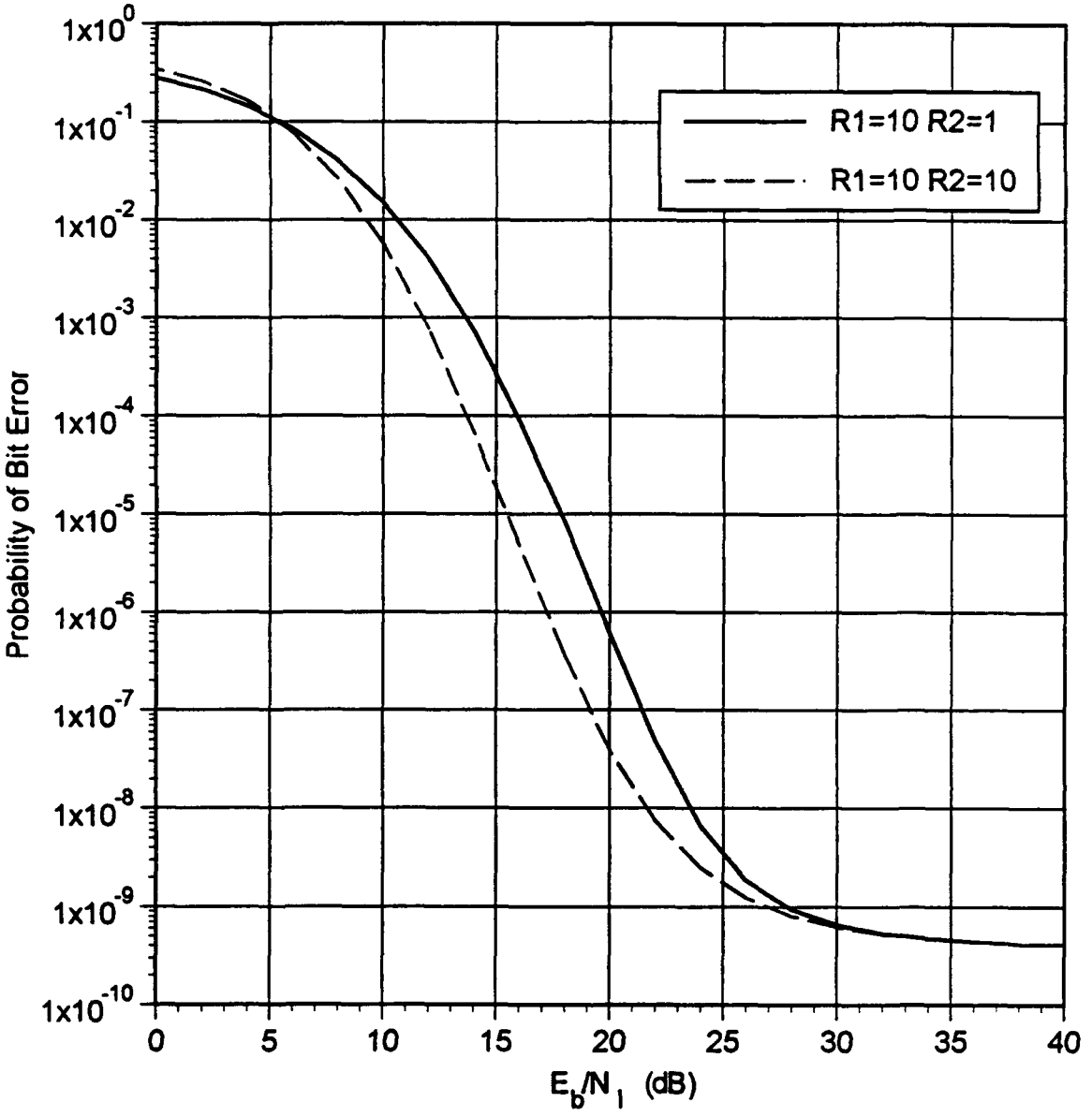

Figure 18. Worst-case receiver performance for a Rician faded signal with Rayleigh and Rician faded interference for $L = 10$, $M = 16$, $E_b/N_0 = 13.35$ dB.

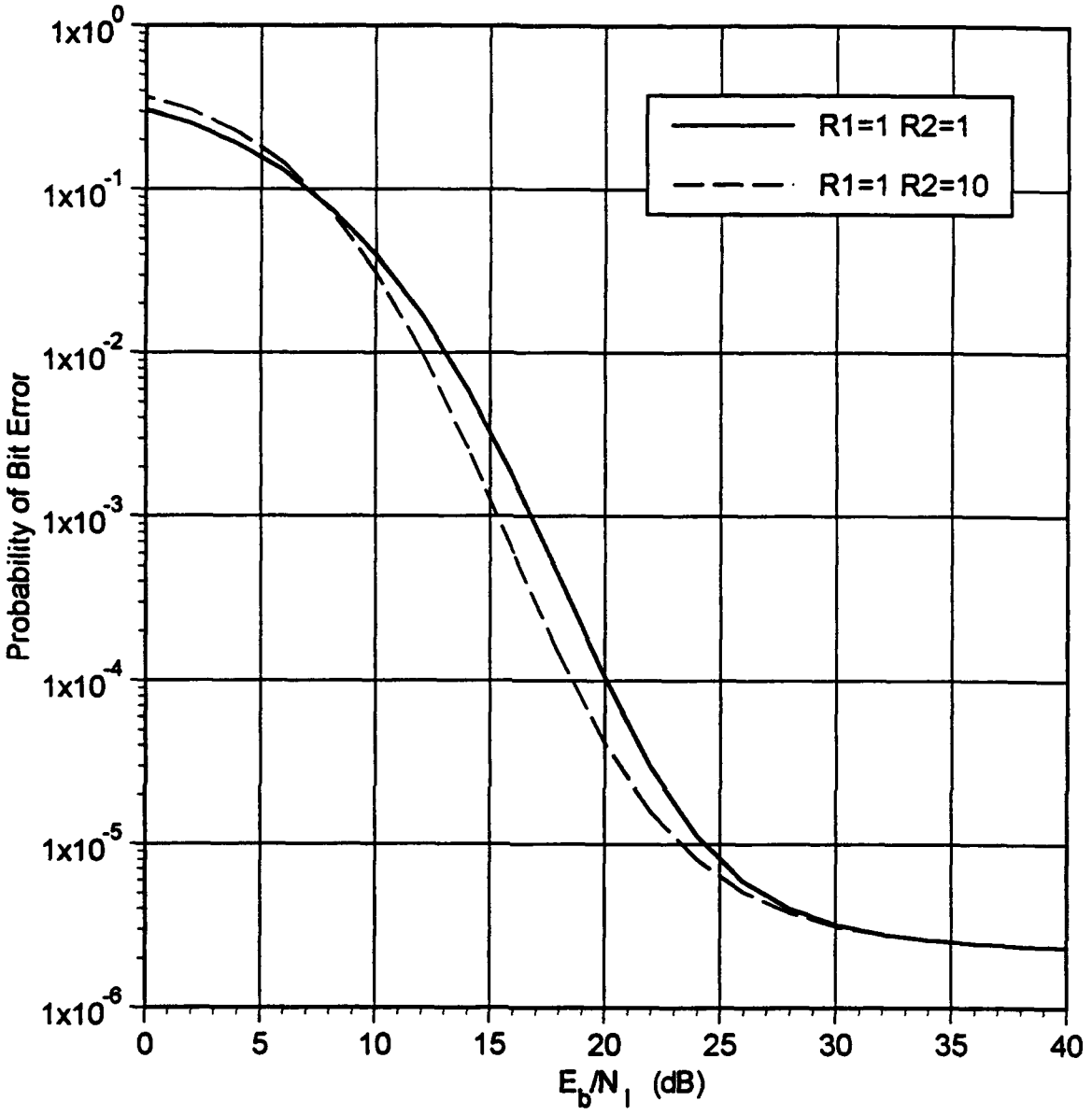

Figure 19. Worst-case receiver performance for a Rayleigh faded signal with Rayleigh and Rician faded interference for $L = 10$, $M = 4$, $E_b/N_0 = 16$ dB.

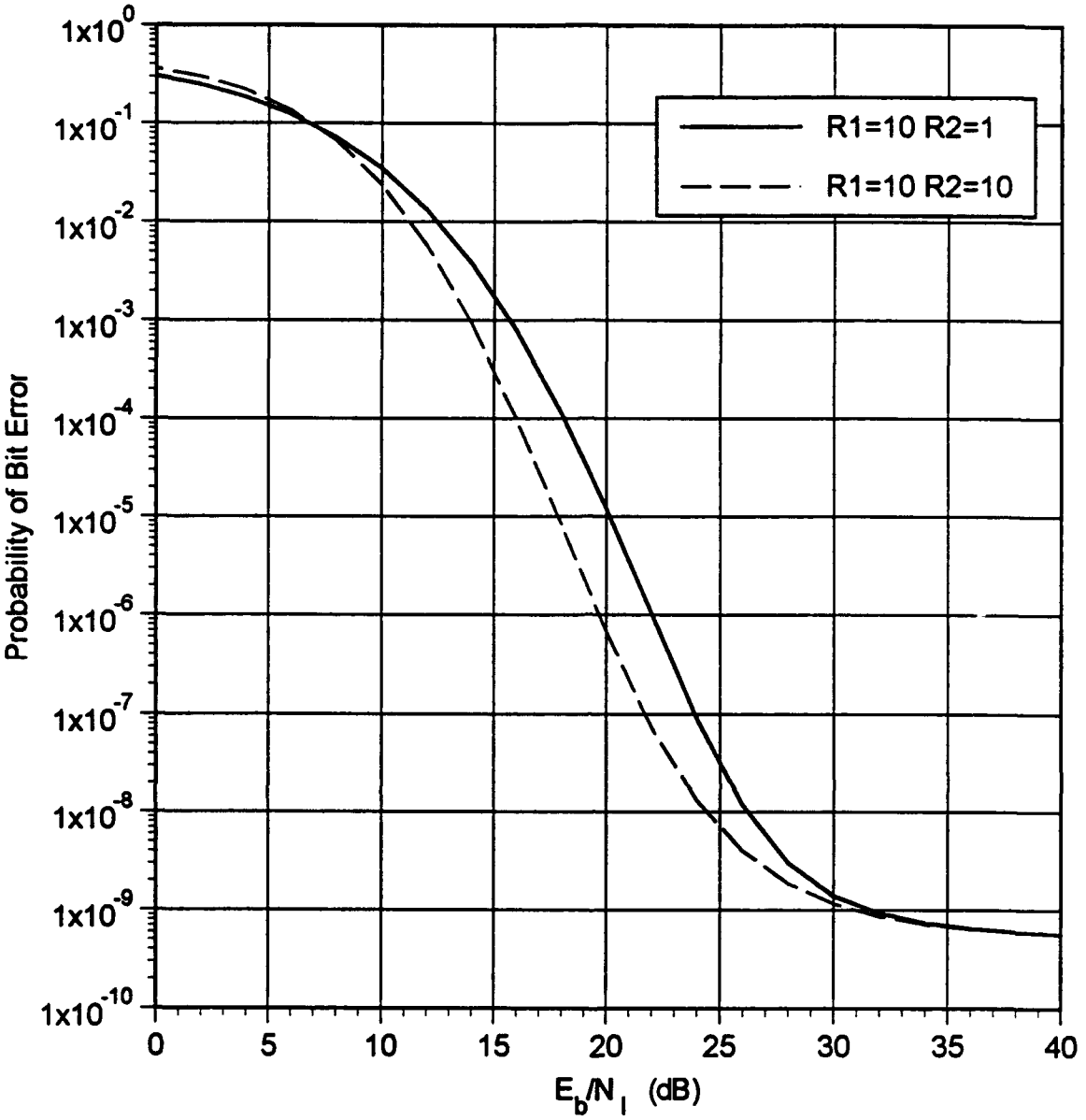

Figure 20. Worst-case receiver performance for a Rician faded signal with Rayleigh and Rician faded interference for $L = 10$, $M = 4$, $E_b/N_0 = 16$ dB.

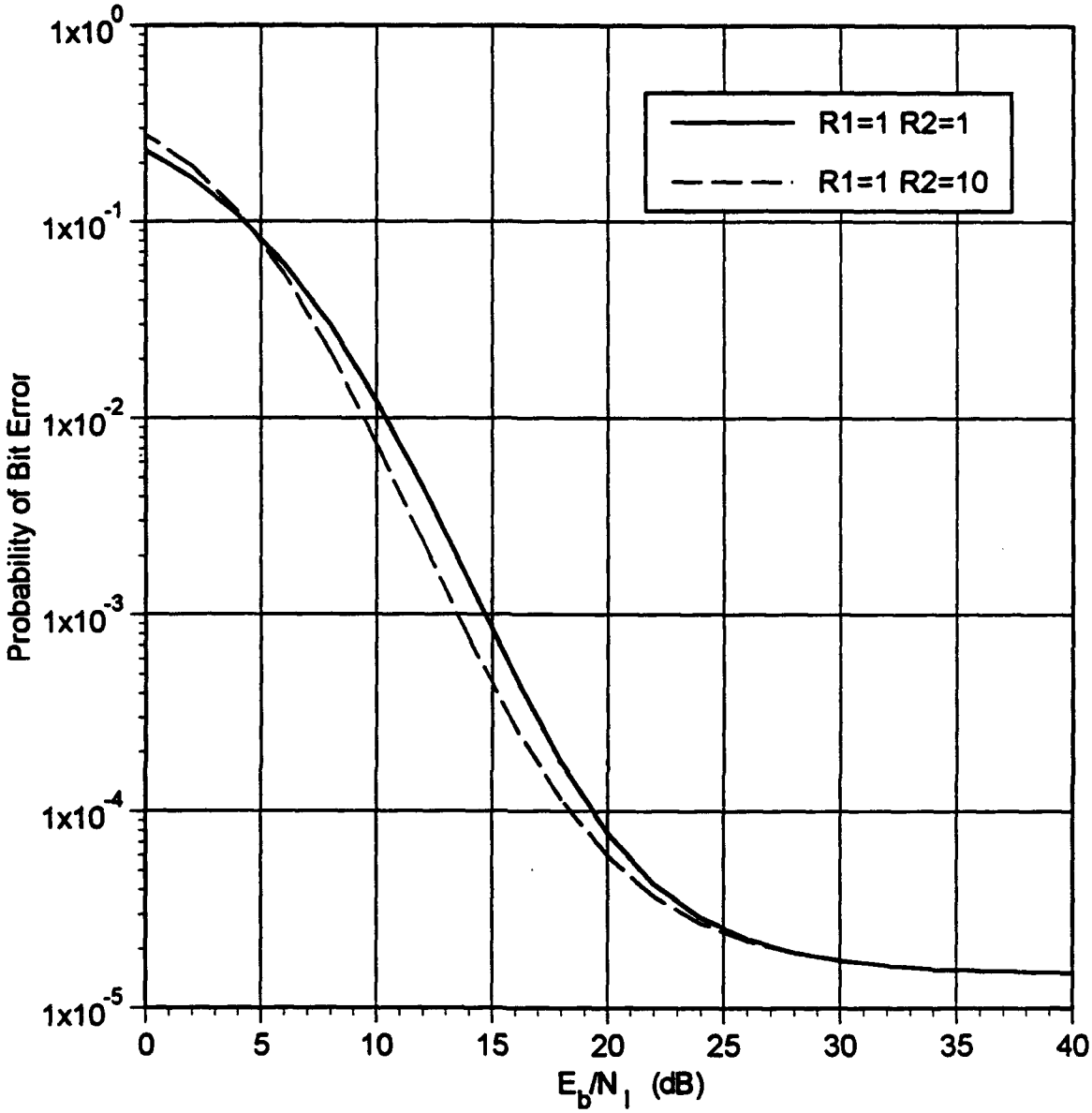

Figure 21. Worst-case receiver performance for a Rayleigh faded signal with Rayleigh and Rician faded interference for $L = 4$, $M = 16$, $E_b/N_0 = 16$ dB.

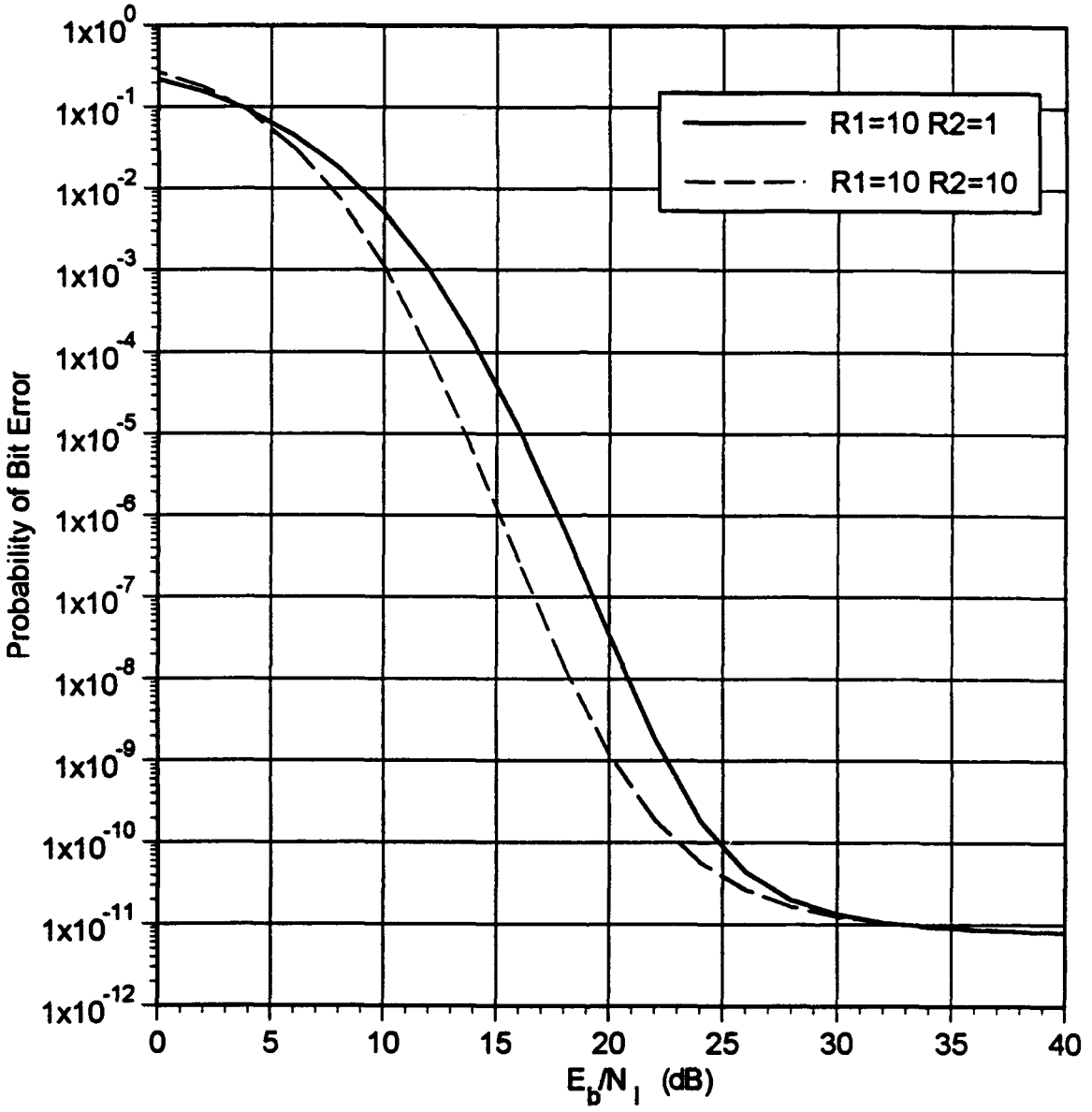

Figure 22. Worst-case receiver performance for a Rician faded signal with Rayleigh and Rician faded interference for $L = 4$, $M = 16$, $E_b/N_0 = 16$ dB.

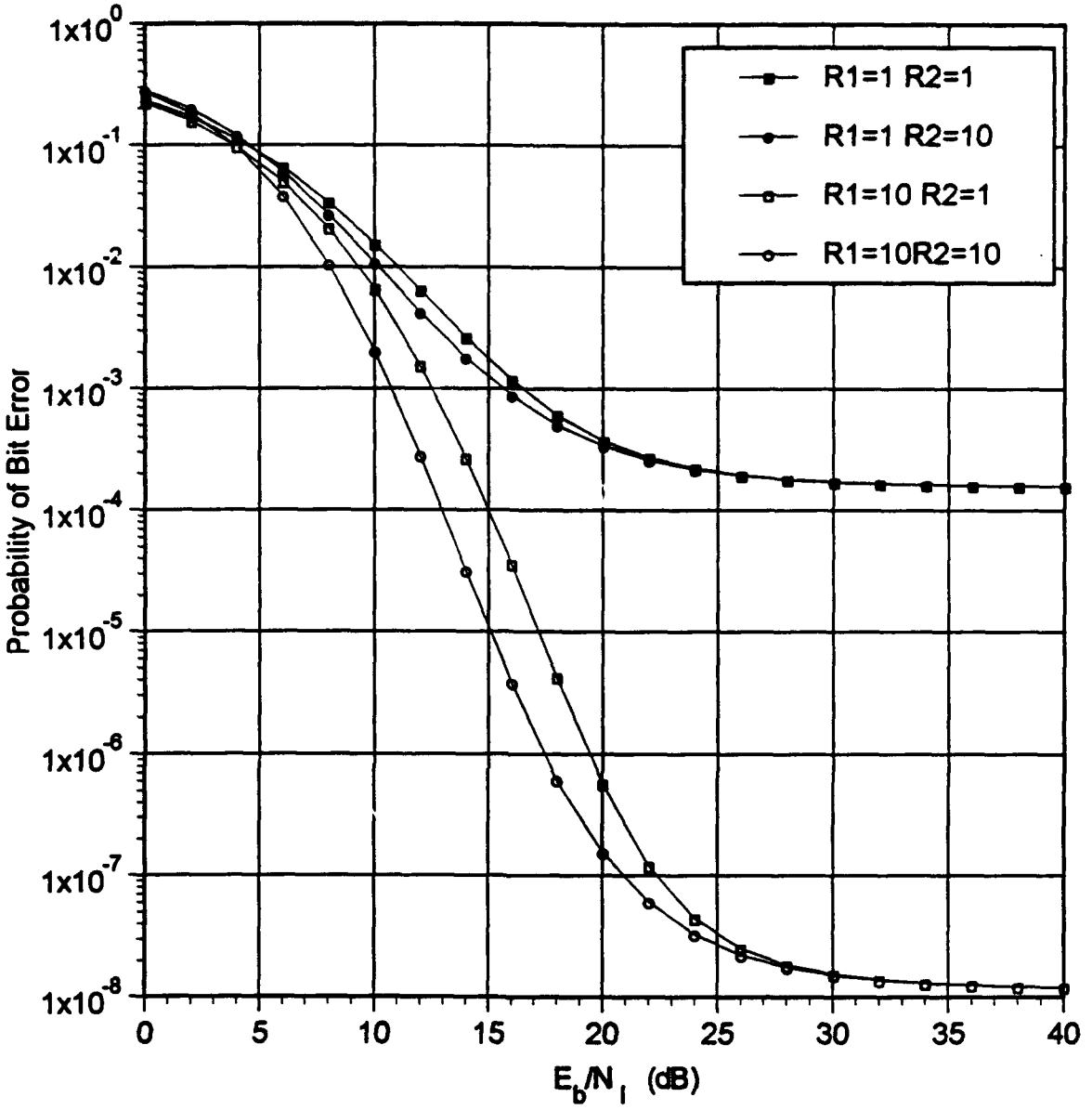

Figure 23. Worst-case receiver performance for a Rayleigh and a Rician faded signal both with Rayleigh and Rician faded interference for $L = 4$, $M = 16$, $E_b/N_0 = 13.35$ dB.

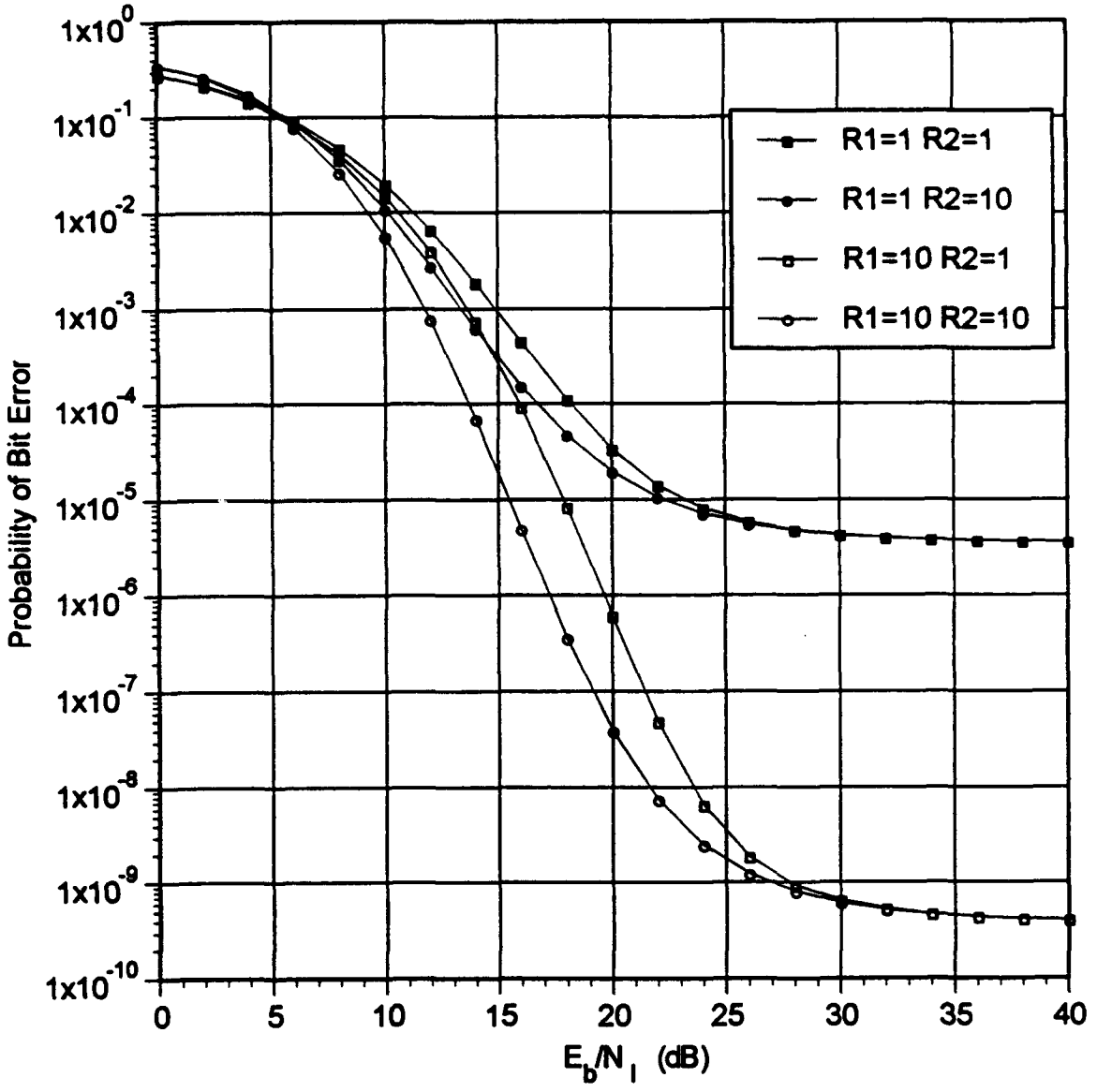

Figure 24. Worst-case receiver performance for a Rayleigh and a Rician faded signal both with Rayleigh and Rician faded interference for $L = 10$, $M = 16$, $E_b/N_0 = 13.35$ dB.

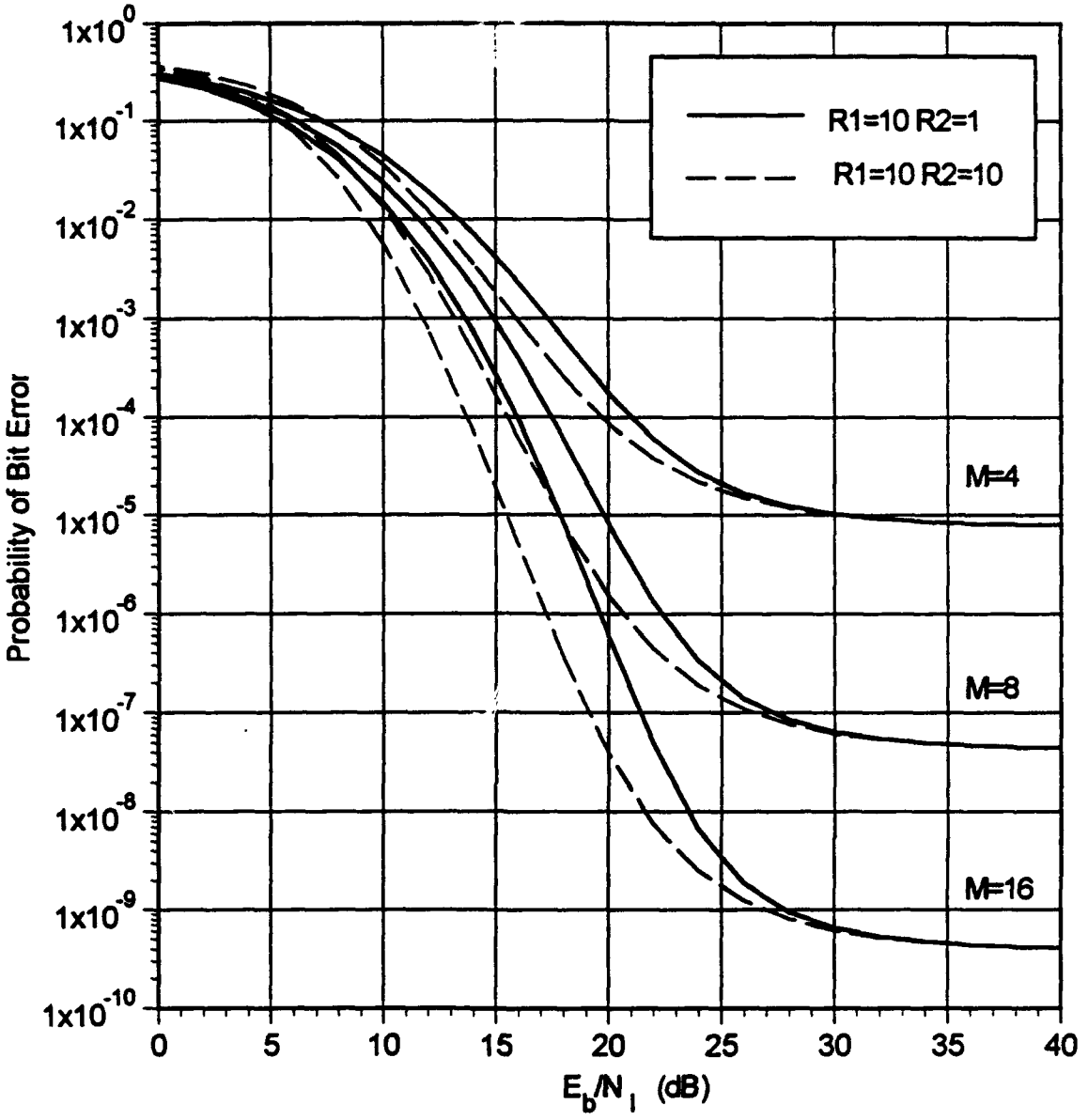

Figure 25. Worst-case receiver performance for modulation orders of $M = 4, 8$, and 16 for a Rician faded signal with Rayleigh and Rician faded interference, $L = 10$ and $E_b/N_0 = 13.35$ dB.

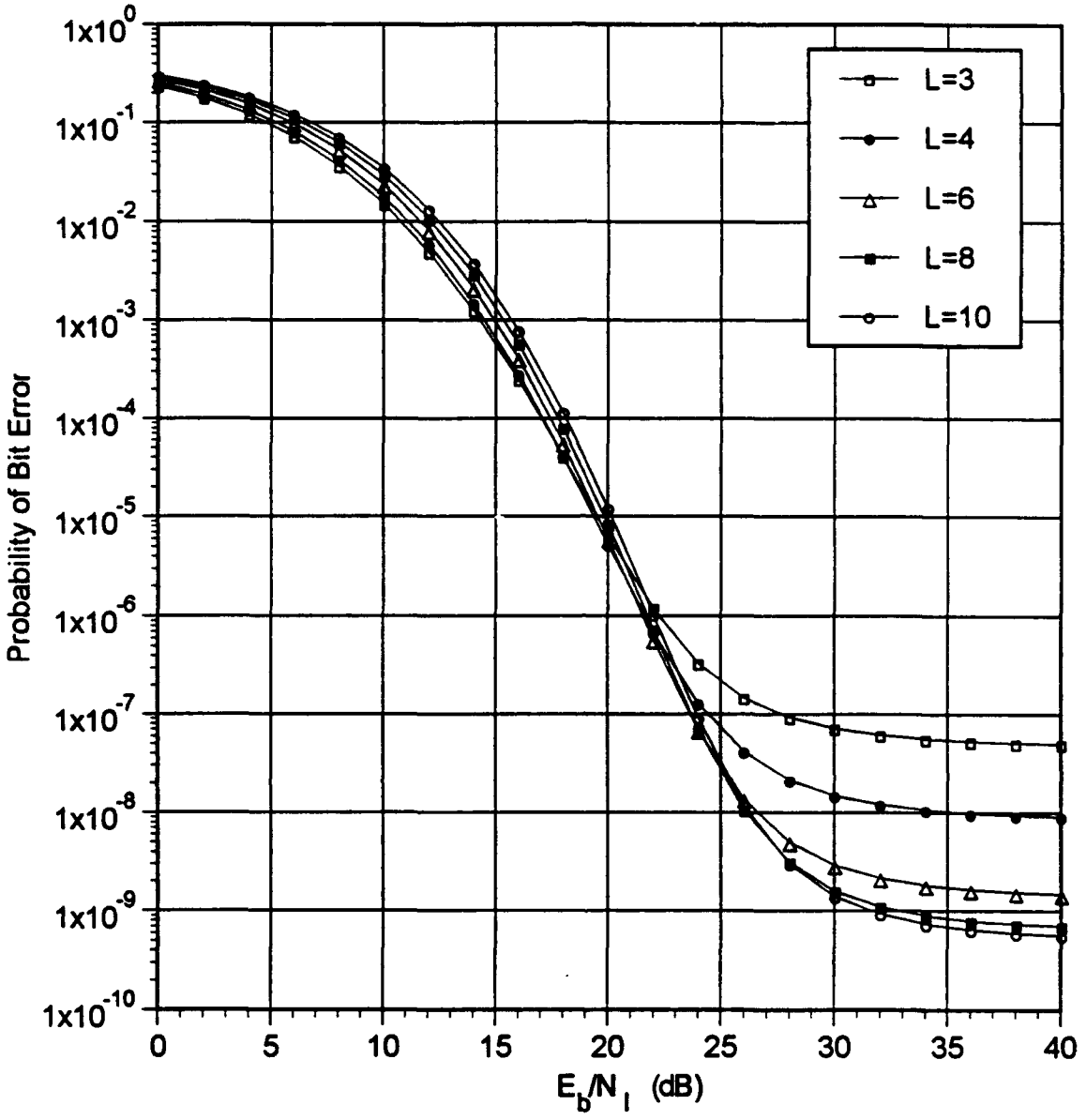

Figure 26. Worst-case receiver performance for diversities of of $L = 3$, 4, 6, 8, and 10 for a Rician faded signal, Rayleigh faded interference, $M = 4$ and $E_b/N_0 = 16$ dB.

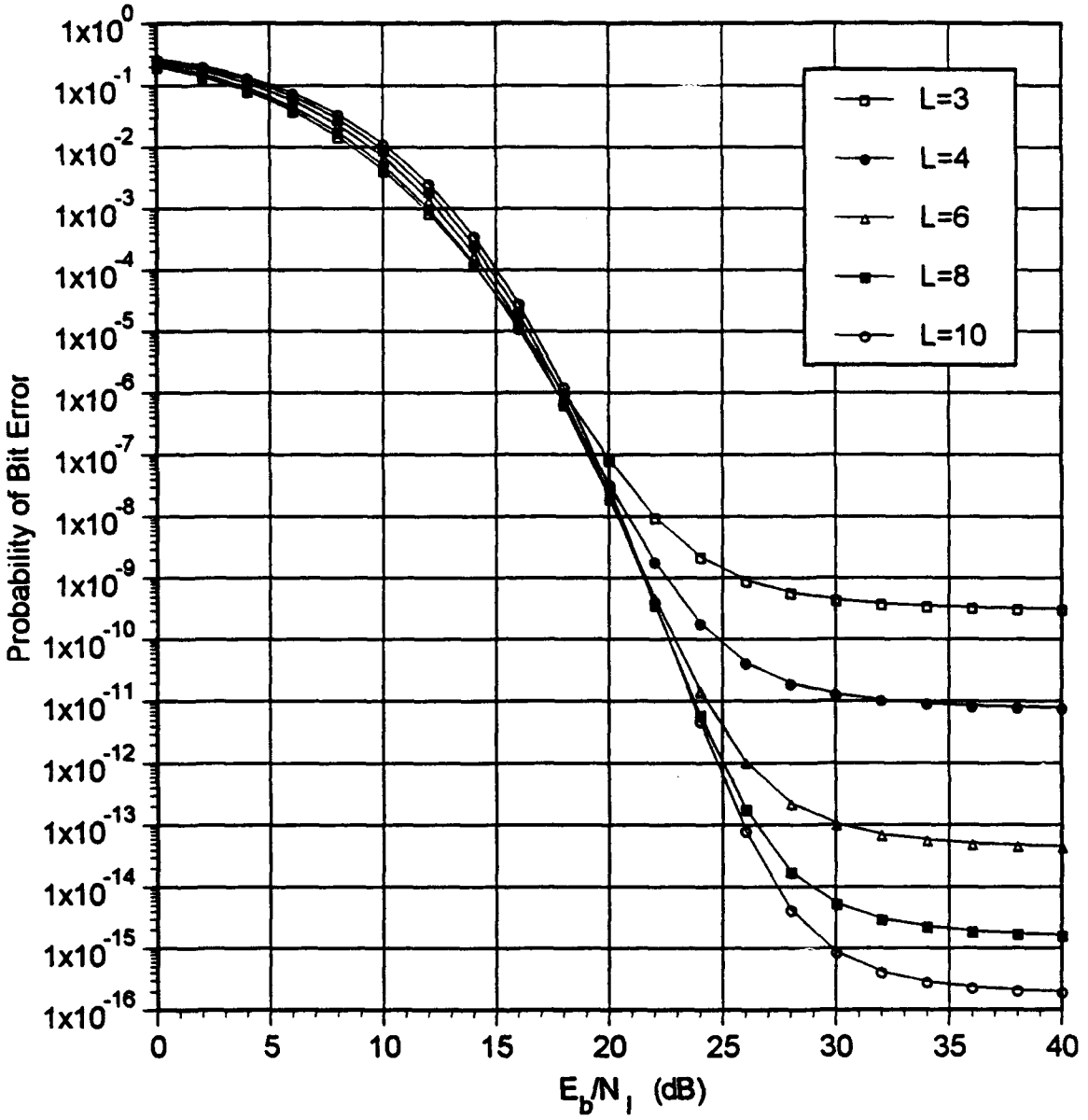

Figure 27. Worst-case receiver performance for diversities of of $L = 3$, 4, 6, 8, and 10 for a Rician faded signal, Rayleigh faded interference, $M = 16$ and $E_b/N_0 = 16$ dB.

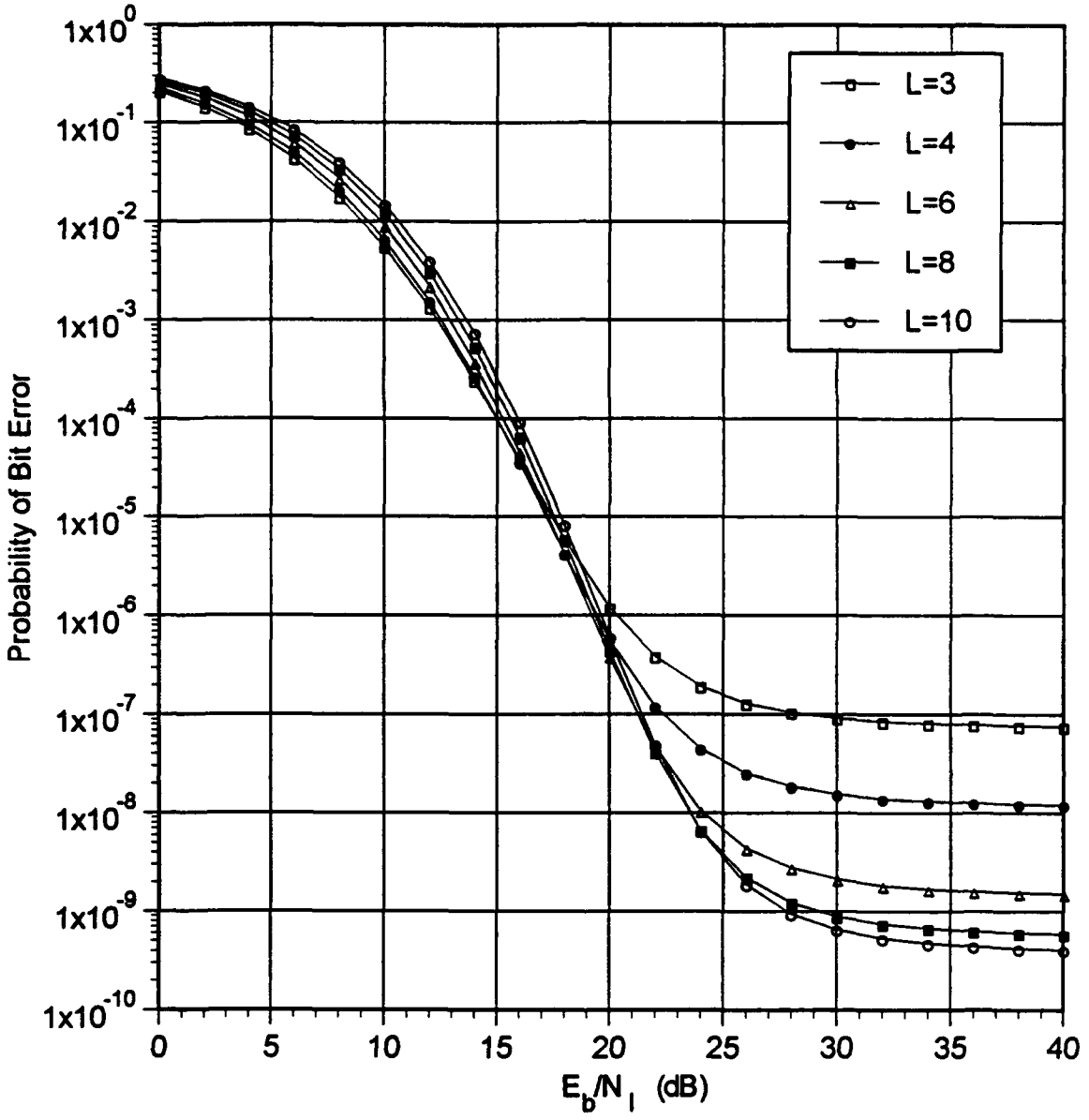

Figure 28. Worst-case receiver performance for diversities of of $L = 3$, 4, 6, 8, and 10 for a Rician faded signal, Rayleigh faded interference, $M = 16$ and $E_b/N_0 = 13.35$ dB.

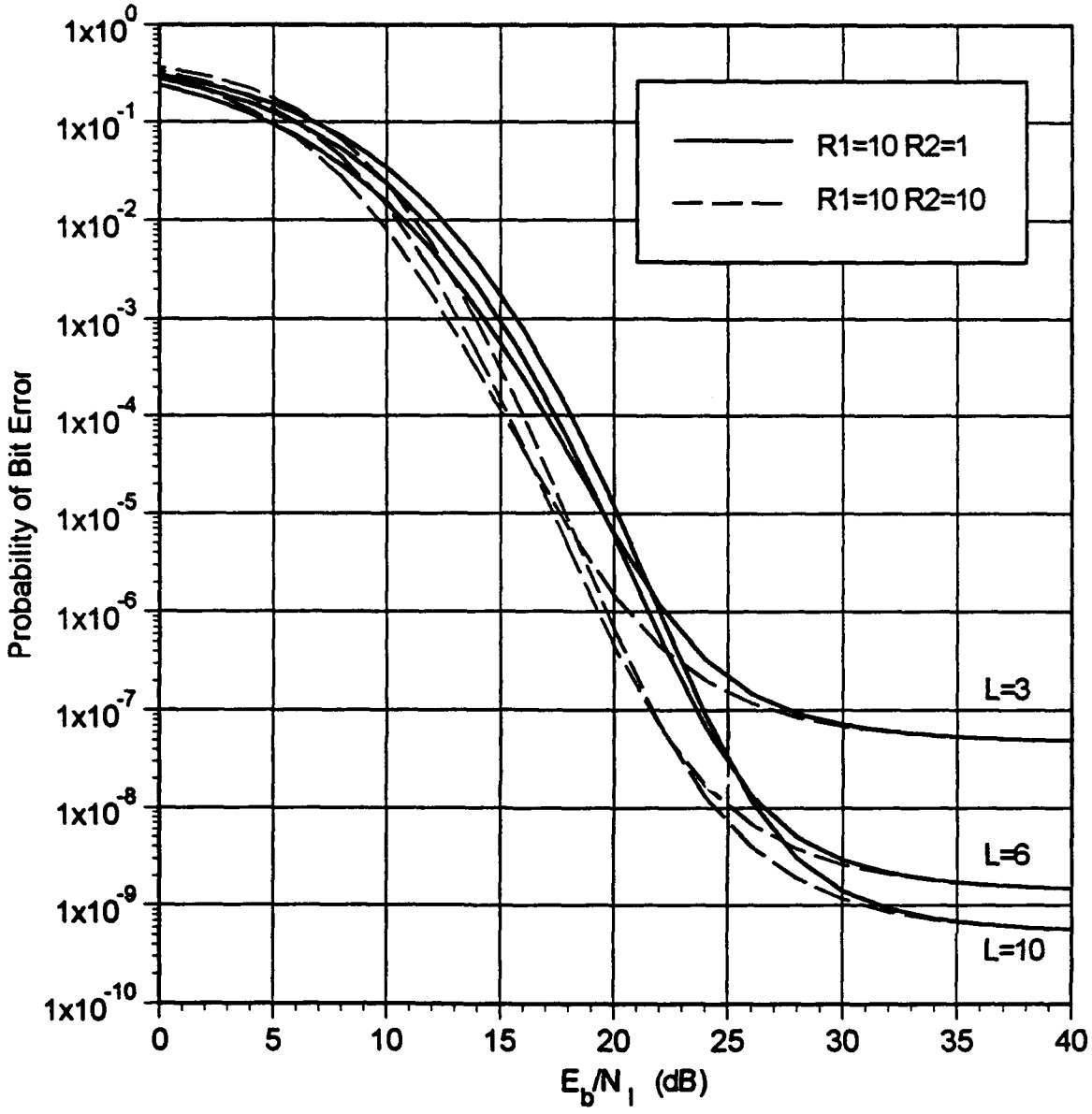

Figure 29. Worst-case receiver performance for diversities of $L = 3$, 6, and 10 for a Rician faded signal with both Rayleigh and Rician faded interference, $M = 4$ and $E_b/N_0 = 16$ dB.

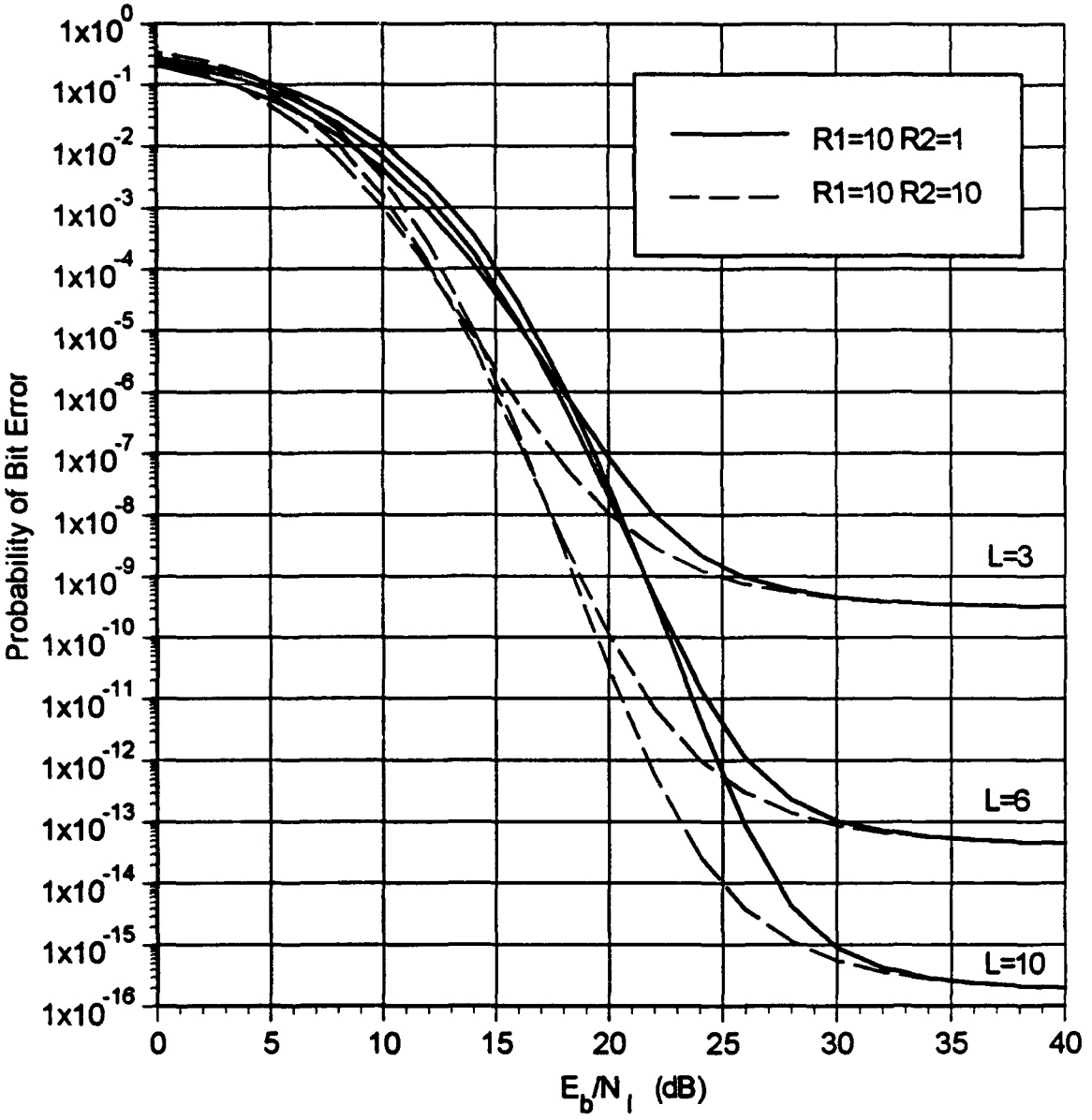

Figure 30. Worst-case receiver performance for diversities of of $L = 3$, 6, and 10 for a Rician faded signal with both Rayleigh and Rician faded interference, $M = 16$ and $E_b/N_0 = 16$ dB.

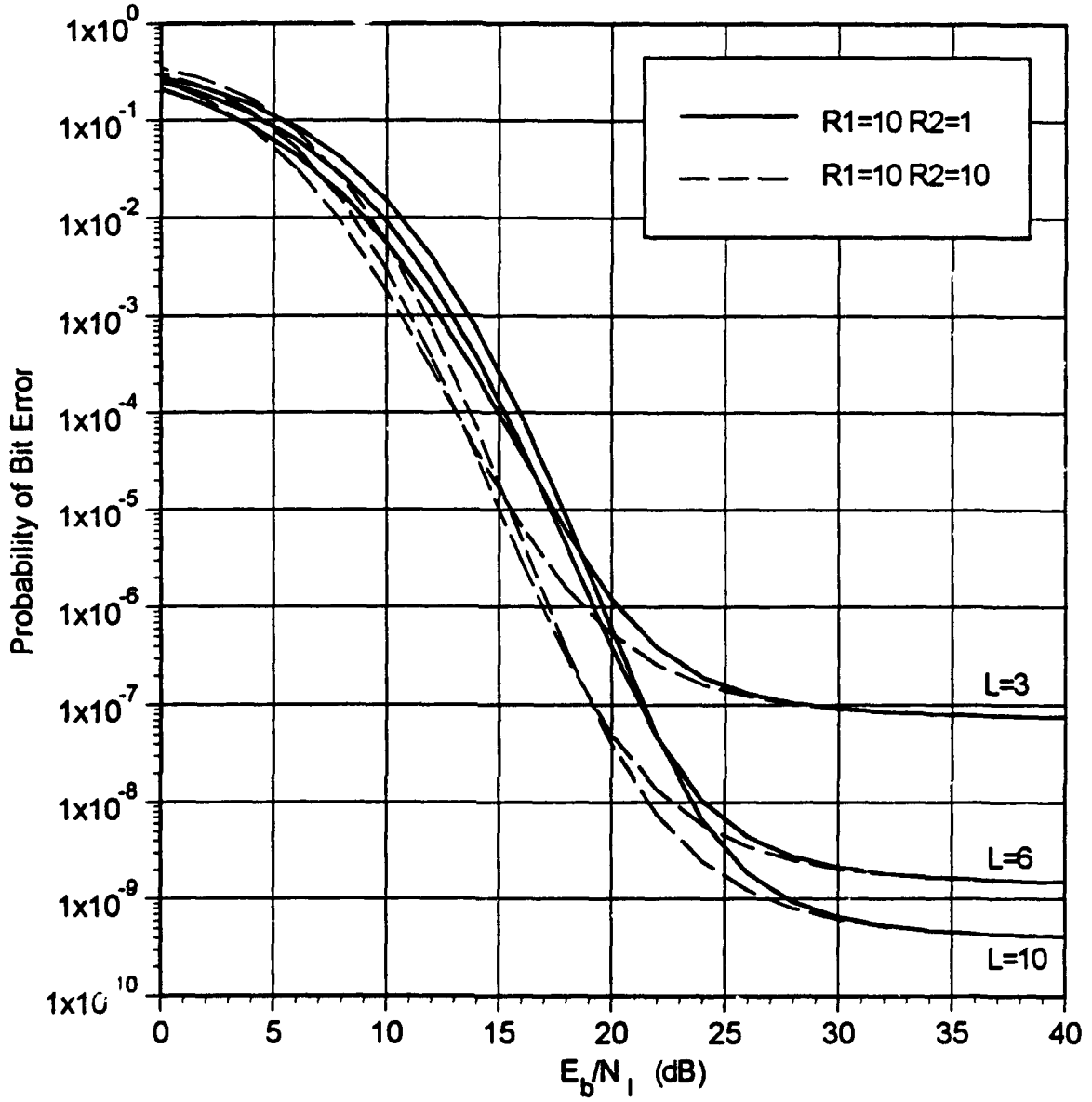

Figure 31. Worst-case receiver performance for diversities of of $L = 3$, 6, and 10 for a Rician faded signal with both Rayleigh and Rician faded interference, $M = 16$ and $E_b/N_0 = 13.35$ dB.

REFERENCES

[1] J. D. Gibson, *Principles Of Digital And Analog Communications*, New York: Macmillan Publishing Company, 1993.

[2] J. G. Proakis, *Communication Systems Engineering*, New Jersey: Prentice Hall, 1994.

[3] D. J. Torrieri, *Principles Of Secure Communication Systems*, Massachusetts: House, 1992.

[4] D. L. Nicholson, *Spread Spectrum Signal Design L.P.E. And A.J. Systems*, Maryland: Computer Science Press, 1988.

[5] R. E. Ziemer and R. L. Peterson, *Digital Communications And Spread Spectrum Systems*, New York: Macmillan Publishing Company, 1985.

[5] R. C. Dixon, *Spread Spectrum Systems*, New York: John Wiley & Sons, 1984.

[6] A. D. Whalen, *Detection of Signals in Noise*, New York: Academic Press, 1971.

[7] J. G. Proakis, *Digital Communications*, 2nd ed., New York: McGraw-Hill, 1989.

[8] R. C. Robertson, "Communication ECCM," class notes from EC 4560, Naval Postgraduate School, Monterey, CA, July 1993.

[9] A. J. Viterbi and I. M. Jacobs, "Advances in coding and modulation for noncoherent channels affected by fading, partial band, and multiple-access interference," in *Advances in Communications Systems, Theory and Applications*, vol. 4, A. J. Viterbi, Ed., Academic Press, 1975.

[10] J. S. Lee, L. E. Miller, and Y. K. Kim, "Probability of error analysis of a BFSK frequency-hopping system with diversity under partial-band jamming interference — Part II: Performance of square-law nonlinear combining soft decision receivers," *IEEE Trans. Commun.*, vol. COM-32, no. 12, pp. 1243–1250, Dec. 1984.

[11] J. S. Lee, L. E. Miller, and R. H. French, "The analyses of uncoded performances for certain ECCM receiver design strategies for multihops/symbol FH/MFSK waveforms," *IEEE J. Select. Areas Commun.*, vol. SAC-3, pp. 611–620, Sept. 1985.

[12] R. C. Robertson and T. T. Ha, "Error probabilities of fast frequency-hopped MFSK with noise-normalization combining in a fading channel with partial-band interference," *IEEE Trans. Commun.*, vol. COM-40, no. 2, pp. 404–412, Feb. 1992.

[13] C. M. Keller and M. B. Pursley, "Diversity combining for channels with fading and partial-band interference," *IEEE J. Select. Areas Commun.*, vol. SAC-5, no. 2, pp. 248–260, Feb. 1987.

[14] C. M. Keller and M. B. Pursley, "Frequency spacing in MFSK frequency-hopped spread spectrum communications over selective fading channels," *Proc. 17th Conf. Inform. Sci. Syst.*, Johns Hopkins Univ., Baltimore, MD, pp. 749–754, Mar. 1983.

[15] A. Papoulis, *Probability, Random Variables, and Stochastic Processes*, 2nd ed., New York: McGraw-Hill, 1984

[16] R. D. Strum and D. E. Kirk, *Comtemporary Linear Systems*, Massachuesetts: PWS Publishing Company, 1994.

[17] I. S. Gradshteyn and I. M. Ryzhik, *Table of Integrals, Series and Products*, San Diego: Academic Press, 1980.

[18] M. Abramowitz and I. A Stugun, *Handbook of Mathematical Functions*, Dover Publication, 1972.

[19] A. Erdelyi, ed., *Tables of Integral Transforms*, vol. I, New York: McGraw-Hill Book Company, Inc., 1954

[20] W. C. Lindsey, "Error probabilities for Rician fading multichannel reception of binary and N-ary signals," *IEEE Trans. on Inform. Theory*, vol. IT-10, pp. 339–350, Oct. 1964.

[21] R. S. Simon, M. T. Stroot, and G. H. Weiss, "Numerical inversion of Laplace transforms with application to percentage labeled mitoses experiments," *Comput. Biomed. Res.*, vol. 5, pp. 596–607, 1972.

[22] R. C. Robertson and K.Y. Lee, "Performance of fast frequency-hopped MFSK receivers with linear and self-normalization combining in a Rician fading channel with partial-band interference," *IEEE J. Select. Areas Commun.*, vol. 10, no. 4, pp. 731–741, May 1992.

[23] T. A. Gulliver and E. Barry Felsead, "Anti-jam by fast FH NCFSK myths and realities," *Proceedings of the IEEE Military Communications Conference*, pp. 187–191, 1993.

INITIAL DISTRIBUTION LIST

		No. Copies
1.	Defense Information Center Cameron Station Alexandria, VA 22304-6145	2
2.	Library Code 52 Naval Postgraduate School Monterey, CA 93943-5000	2
3.	Chairman, Code EC Department of Electrical and Computer Engineering Naval Postgraduate School Monterey, CA 93943-5000	1
4.	Professor R. Clark Robertson, Code EC/Rc Department of Electrical and Computer Engineering Naval Postgraduate School Monterey, CA 93943-5000	3
5.	Professor Ron J. Pieper, Code EC/Pr Department of Electrical and Computer Engineering Naval Postgraduate School Monterey, CA 93943-5000	1
6.	Melody Kragh 102 Malloway Lane Monterey, CA 93940	3